Available online at www.sciencedirect.com
SCIENCE DIRECT®
Journal of Molecular Spectroscopy 236 (2006) 75–90
Journal of MOLECULAR SPECTROSCOPY
www.elsevier.com/locate/jms

Room-temperature broadening and pressure-shift coefficients in the v_2 band of CH_3D–O_2: Measurements and semi-classical calculations

Adriana Predoi-Cross [a,*], Kyle Hambrook [a], Shannon Brawley-Tremblay [a], Jean-Pierre Bouanich [b], V. Malathy Devi [c], Mary Ann H. Smith [d]

[a] Physics Department, University of Lethbridge, 4401 University Drive, Lethbridge, Alta., Canada T1K 3M4
[b] Laboratoire de Photophysique Moléculaire, CNRS UPR3361, Université de Paris-Sud, Bâtiment 350, F-91405 Orsay, France
[c] Department of Physics, The College of William and Mary, Box 8795, Williamsburg, VA 23187-8795, USA
[d] Science Directorate, NASA Langley Research Center, MS 401A, Hampton, VA 23681-2199, USA

Received 1 December 2005; in revised form 16 December 2005
Available online 15 February 2006

Abstract

We report measured Lorentz O_2-broadening and O_2-induced pressure-shift coefficients of CH_3D in the v_2 fundamental band. Using a multispectrum fitting technique we have analyzed 11 laboratory absorption spectra recorded at 0.011 cm^{-1} resolution using the McMath–Pierce Fourier transform spectrometer, Kitt Peak, Arizona. Two absorption cells with path lengths of 10.2 and 25 cm were used to record the spectra. The total sample pressures ranged from 0.98 to 339.85 Torr with CH_3D volume mixing ratios of 0.012 in oxygen. We report measurements for O_2 pressure-broadening coefficients of 320 v_2 transitions with quantum numbers as high as $J'' = 17$ and $K = 14$, where $K'' = K' \equiv K$ (for a parallel band). The measured O_2-broadening coefficients range from 0.0153 to 0.0645 cm^{-1} atm^{-1} at 296 K. All the measured pressure-shifts are negative. The reported O_2-induced pressure-shift coefficients vary from about -0.0017 to -0.0068 cm^{-1} atm^{-1}. We have examined the dependence of the measured broadening and shift parameters on the J'', and K quantum numbers and also developed empirical expressions to describe the broadening coefficients in terms of m ($m = -J''$, J'', and $J'' + 1$ in the ${}^QP$-, ${}^QQ$-, and ${}^QR$-branch, respectively) and K. On average, the empirical expressions reproduce the measured broadening coefficients to within 4.4%. The O_2-broadening and pressure shift coefficients were calculated on the basis of a semiclassical model of interacting linear molecules performed by considering in addition to the electrostatic contributions the atom–atom Lennard-Jones potential. The theoretical results of the broadening coefficients are generally larger than the experimental data. Using for the trajectory model an isotropic Lennard-Jones potential derived from molecular parameters instead of the spherical average of the atom–atom model, a better agreement is obtained with these data, especially for $|m| \leqslant 12$ values (11.3% for the first calculation and 8.1% for the second calculation). The O_2-pressure shifts whose vibrational contribution are either derived from parameters fitted in the ${}^QQ$-branch of self-induced shifts of CH_3D or those obtained from pressure shifts induced by Xe in the v_3 band of CH_3D are in reasonable agreement with the scattered experimental data (17.0% for the first calculation and 18.7% for the second calculation).

Keywords: Monodeuterated methane; CH_3D; O_2-broadening; Fourier transform infrared spectroscopy; Spectral lineshape; Semi-classical calculation

1. Introduction

Laboratory spectroscopic studies of the v_2 vibrational band of CH_3D are needed for the correct interpretation of Earth's atmospheric spectra. The v_2 band of CH_3D is the lowest band ($v_0 \approx 2200$ cm^{-1}) of a polyad of nine interacting vibrational states. This paper is a continuation of our study of spectroscopic line parameters in this fundamental band [1,2]. Few measurements and calculations of O_2-broadening coefficients for CH_3D have been published and they refer only to the v_3 fundamental [3,4]. To the best

* Corresponding author. Fax: +1 403 329 2057.
E-mail address: Adriana.predoicross@uleth.ca (A. Predoi-Cross).

0022-2852/$ - see front matter © 2005 Elsevier Inc. All rights reserved.
doi:10.1016/j.jms.2005.12.012

of our knowledge, no prior measurements of O_2-induced pressure shift coefficients have been made.

Several theoretical efforts concerned with O_2-broadening coefficients of CH_3D have been put forth. Tejwani and Fox [5] calculated N_2-, O_2-, self-, and H_2-broadening coefficients for CH_3D using the Anderson–Tsao–Curnutte (ATC) theory by considering only the electrostatic interaction between the quadrupole moment of the perturber and the octople moment of CH_3D, with an effective value of this octopole moment strongly overestimated (5.6 D Å^2, instead of 3.1 D Å^2 in this study). They have computed pressure-broadening coefficients for the above broadening gases for a wide range of J and K values as well as the temperature dependence of the pressure-broadening coefficients in the 100–300 K range. The O_2-broadening coefficients of CH_3D in the ν_3 band reported in [3] were calculated using the theoretical model developed in [6]. For the intermolecular potential a simple formulation with two adjustable parameters [7] corresponding to dispersion, induction, and repulsive contributions has been used in addition to the electrostatic interactions. Although the calculated results are generally in reasonable agreement with the experimental data, except at high J values where they are underestimated, the two adjustable potential parameters used have probably no physical meaning. Here, we consider a different theoretical approach for the calculation of broadening coefficients that was recently applied to CH_3D self-perturbed [1], CH_3D–H_2 [8], and CH_3D–N_2 [2] without any adjustable parameters. CH_3D is approximated as a linear molecule for its interactions with O_2 and the potential involves the atom–atom Lennard-Jones model [9] in addition to the electrostatic contributions. The theoretical formulation is similar to that described previously [2] and only some features and characteristics of the potential used will be briefly presented.

2. Experimental details

The 11 absorption spectra used in this work were recorded at an unapodized resolution of 0.0056 cm^{-1} using the McMath-Pierce Fourier transform spectrometer (FTS) of the National Solar Observatory (NSO) on Kitt Peak. Two absorption cells with path lengths of 10.2 and 25 cm were used in the experiments. The spectra covering the 2048–2318 cm^{-1} were simultaneously fit in segments of 5–10 cm^{-1} wavenumber intervals using a multispectrum nonlinear least-squares procedure [10]. This analysis tool allowed us to combine spectra recorded with low pressures of 98% pure CH_3D, self-broadened spectra, and lean mixtures (~1%) of CH_3D in O_2 in a single least-squares solution. The experimental conditions for each spectrum are presented in Table 1. The experimental setup and data reduction methods were described in detail in our earlier study [1]. Residual water vapor lines appeared in all of our spectra as a combination of low pressure absorption due to small amounts (50 mTorr) of residual water vapor present in the vacuum tank enclosing the FTS, and H_2O absorption arising from water vapor in the N_2-purged atmospheric paths between the source and the absorption cell and between the absorption cell and the entrance aperture of the interferometer. The wavenumber calibration for the CH_3D line positions was performed with respect to the well-known line centers [11] of residual water lines.

An example of a multispectrum fitted interval is presented in Fig. 1. The top panel shows 11 overlaid spectra of ^QR-branch transitions with $J'' = 11$ and K values from 0 to 10. The bottom panel indicates the fit residuals (observed minus calculated for all 11 spectra). The positions of transitions due to contaminants such as residual CO were determined prior to using the multispectrum fitting procedure. During the analysis these lines were included in the least-squares solution using 0.075 cm^{-1} atm^{-1} at 296 K as O_2-broadening and -0.005 cm^{-1} atm^{-1} as O_2-induced pressure shift coefficients, respectively.

3. Results and discussion

The results of our multispectrum analysis are presented in Table 2. The O_2-broadening coefficients for CH_3D transitions in the ν_2 band are given in units of cm^{-1} atm^{-1} at 296 K. For each transition we list the line center positions retrieved from the fits (in cm^{-1}) and the transitions

Table 1
Experimental conditions for the spectra using in this study

Temperature (K)	Broadening gas	$^{12}CH_3D$ volume mixing ratio	Path (cm)	Pressure (Torr)
300.20	$^{12}CH_3D$	1.00	10.2	0.98
300.00	$^{12}CH_3D$	1.00	10.2	2.95
300.90	$^{12}CH_3D$	1.00	10.2	17.50
300.70	$^{12}CH_3D$	1.00	10.2	79.00
300.20	$^{12}CH_3D$	1.00	10.2	110.00
299.80	$^{12}CH_3D$	1.00	10.2	152.00
299.80	$^{12}CH_3D$	1.00	10.2	303.00
295.90	O_2	~0.012	25.0	339.85
295.65	O_2	~0.012	25.0	302.50
295.45	O_2	~0.012	25.0	202.35
295.45	O_2	~0.012	25.0	102.40

Note. 760 Torr = 1 atm = 101.325 kPa.

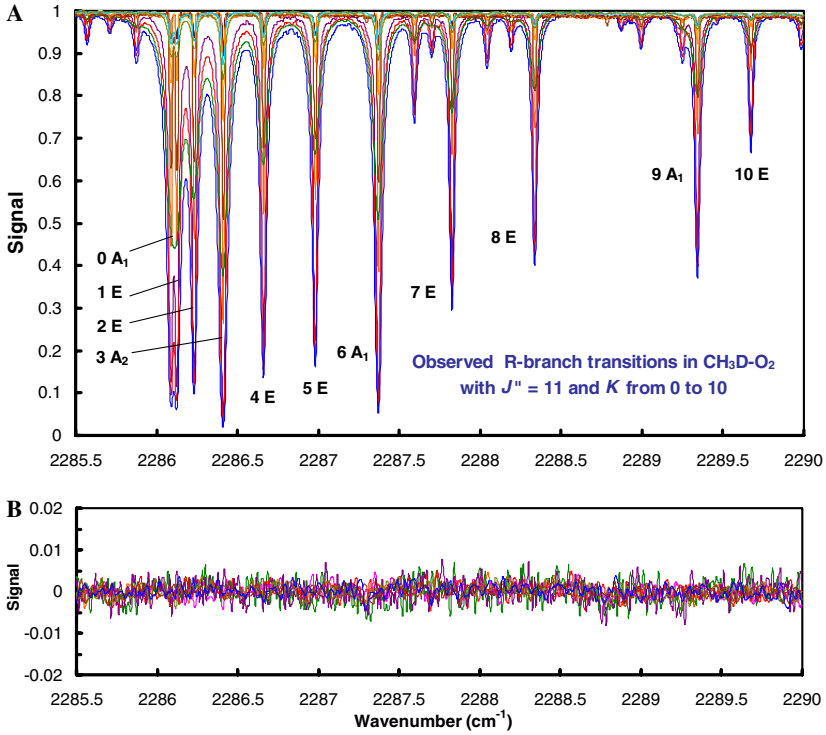

Fig. 1. An example of a multispectrum fitted interval in the R-branch of the ν_2 band of $^{12}CH_3D$–O_2. All experimental spectra are overlaid in (A). (B) The (observed − calculated) fit residuals are plotted.

quantum numbers. In our analysis we have not applied any temperature corrections to the measured pressure-shift coefficients. Hence, the O_2-pressure induced shift coefficients listed in Table 2 correspond to values at the mean temperature (298 ± 2 K) at which the spectra were recorded. The spectroscopic results are arranged in groups of ^{Q}P-, ^{Q}Q-, and ^{Q}R-branches. Within each branch, the results are arranged separately for the A- and E-species transitions. In Table 2 the errors quoted in parentheses represent one standard deviation uncertainties in the measured quantities in units of the last quoted digit.

3.1. Discussion of the measured O_2-broadening coefficients

The measured O_2-broadening coefficients, $\gamma(O_2)$, have been plotted as a function of m ($m = -J''$, J'', $J''+1$ for ^{Q}P-, ^{Q}Q-, and ^{Q}R-branch lines, respectively) and are presented in Fig. 2. The unique pattern of the O_2-broadening coefficients for ^{Q}Q-branch transitions with $J'' = K$ has been highlighted with a different symbol. In Fig. 3 we have plotted the ratio of our measured O_2-broadening coefficients to broadening coefficients from the ν_3 band reported in [3]. The mean ratio of O_2-broadening coefficients is 1.00(4) highlighting the very good agreement between our O_2-broadening coefficients and transitions with the same quantum numbers and symmetry species of the ν_3 band [3].

We have fitted the experimental O_2-broadening coefficients to empirical expressions as previously done in [1,2]. The broadening coefficients for all transitions except $J'' = K$ and $J'' = K+1$ in the ^{Q}Q-branch, were fitted to the following expression:

$$\gamma(O_2) = c_0 + c_1|m|(|m|+1) + c_2K^2. \quad (1)$$

$\gamma(O_2)$ is expressed in cm^{-1} atm^{-1} at 296 K. The constants c_0, c_1, and c_2 were determined by a least-squares fit to the present measured broadening coefficients and are given in Table 3. For the fit with 300 lines, the average percentage difference between the experimental and calculated broadening coefficients (using Eq. (1) and parameters in Table 3) is 4.5%.

In the ^{Q}Q-branch for the $J'' = K$ transitions the broadening coefficients were expressed as

$$\gamma = c_0 + c_1|m|(|m|+1) + c_2|m|^2(|m|+1)^2. \quad (2)$$

As again determined by a least-squares fit to the data, the constants c_0, c_1, and c_2 are also given in Table 3. The average percentage difference between the experimental and calculated broadening coefficients (using Eq. (2) and parameters in Table 3) for the fit with 11 transitions is 2.5%.

We noticed that the ^{Q}Q-branch transitions with the $J'' = K+1$ also follow a distinctive pattern and have fitted them to Eq. (2). The c_0, c_1, and c_2 constants for this last fit are also given in Table 3. The percentage difference between the experimental and calculated broadening coefficients (using Eq. (2) and parameters in Table 3) for the fit with nine transitions with the $J'' = K+1$ is 2.1%. Overall, on average the empirical expressions reproduce the measured broadening coefficients to 4.4%.

Table 2
Measured zero-pressure line positions, O_2-broadening coefficients, and O_2-induced pressure-shift coefficients in the ν_2 band of CH_3D

Position[a,b]	J'	K'	N'	J''	K''	N''	Assignment	Measured $\gamma(O_2)$[a,c]	Measured $\delta(O_2)$[a,d]	Calc. 1 $\gamma(O_2)$[c]	Calc. 1 $\delta(O_2)$[c]	Calc. 2 $\gamma(O_2)$[c]	Calc. 2 $\delta(O_2)$[c]
2066.273056(25)	15	0	A2	16	0	A1	QP(16,0,A1)	0.0448(10)		0.0464	−0.00562	0.0381	−0.00442
2066.657099(26)	15	3	A2	16	3	A1	QP(16,3,A1)	0.0452(14)		0.047	−0.00565	0.0387	−0.00445
2070.022672(64)	15	9	A2	16	9	A1	QP(16,9,A1)	0.0387(2)	−0.00551(23)	0.0496	−0.00559	0.0411	−0.00447
2075.615162(16)	14	3	A2	15	3	A1	QP(15,3,A1)	0.0464(10)		0.0489	−0.00556	0.0409	−0.00440
2076.758022(19)	14	6	A2	15	6	A1	QP(15,6,A1)	0.0422(6)		0.0503	−0.00552	0.0422	−0.00441
2078.961676(27)	14	9	A2	15	9	A1	QP(15,9,A1)	0.0415(2)		0.0511	−0.00554	0.0427	−0.00446
2084.107187(46)	13	0	A2	14	0	A1	QP(14,0,A1)	0.0524(2)		0.0502	−0.00545	0.0425	−0.00433
2084.488001(27)	13	3	A2	14	3	A1	QP(14,3,A1)	0.0457(2)	−0.00435(17)	0.0508	−0.00547	0.0431	−0.00436
2087.831176(48)	13	9	A2	14	9	A1	QP(14,9,A1)	0.0420(2)	−0.00540(14)	0.0523	−0.00551	0.0440	−0.00446
2094.404257(28)	12	6	A2	13	6	A1	QP(13,6,A1)	0.0422(2)		0.0537	−0.00536	0.0461	−0.00433
2096.654013(45)	12	9	A2	13	9	A1	QP(13,9,A1)	0.0448(6)	−0.00534(12)	0.0532	−0.00550	0.0449	−0.00447
2101.614611(28)	11	0	A2	12	0	A1	QP(12,0,A1)	0.0518(2)	−0.00634(10)	0.0539	−0.00528	0.0469	−0.00425
2101.988972(18)	11	3	A2	12	3	A1	QP(12,3,A1)	0.0467(4)	−0.00358(3)	0.0544	−0.00529	0.0473	−0.00428
2103.105139(23)	11	6	A2	12	6	A1	QP(12,6,A1)	0.0444(5)	−0.00440(13)	0.0552	−0.00528	0.0479	−0.00430
2105.492353(35)	11	9	A2	12	9	A1	QP(12,9,A1)	0.0489(10)	−0.00579(26)	0.0537	−0.00554	0.0451	−0.00452
2111.726664(19)	10	6	A2	11	6	A1	QP(11,6,A1)	0.0461(3)	−0.00495(2)	0.0566	−0.00522	0.0493	−0.00427
2113.320480(59)	10	9	A2	11	9	A1	QP(11,9,A1)	0.0486(3)		0.0532	−0.00569	0.0439	−0.00465
2118.805485(56)	9	0	A2	10	0	A1	QP(10,0,A1)	0.0556(2)	−0.00576(14)	0.0574	−0.00509	0.0509	−0.00415
2119.173122(41)	9	3	A2	10	3	A1	QP(10,3,A1)	0.0468(2)	−0.00396(16)	0.0577	−0.00510	0.0512	−0.00417
2120.269633(13)	9	6	A2	10	6	A1	QP(10,6,A1)	0.0484(3)	−0.00400(2)	0.0577	−0.00518	0.0504	−0.00426
2135.684242(16)	7	0	A2	8	0	A1	QP(2,0,A1)	0.0575(2)	−0.00385(6)	0.0607	−0.00489	0.0546	−0.00403
2136.045320(19)	7	3	A2	8	3	A1	QP(2,3,A1)	0.0552(2)	−0.00487(6)	0.0607	−0.00492	0.0544	−0.00406
2152.251052(21)	5	0	A2	6	0	A1	QP(6,0,A1)	0.0591(4)	−0.00522(12)	0.0635	−0.00469	0.0576	−0.00389
2152.605736(13)	5	3	A2	6	3	A1	QP(6,3,A1)	0.0583(3)	−0.00414(5)	0.0628	−0.00475	0.0564	−0.00394
2168.503061(15)	3	0	A2	4	0	A1	QP(4,0,A1)	0.0616(3)	−0.00416(2)	0.0655	−0.00439	0.0595	−0.00367
2184.434681(28)	1	0	A2	2	0	A1	QP(2,0,A1)	0.0645(6)	−0.00372(14)	0.0668	−0.00467	0.0608	−0.00404
2057.228673(29)	16	0	A1	17	0	A2	QP(17,0,A2)	0.0475(10)		0.0444	−0.00571	0.0358	−0.00445
2057.611958(28)	16	3	A1	17	3	A2	QP(17,3,A2)	0.0451(15)		0.0451	−0.00573	0.0365	−0.00449
2058.771359(30)	16	6	A1	17	6	A2	QP(17,6,A2)	0.0391(11)		0.0466	−0.00568	0.0380	−0.00448
2067.808757(20)	15	6	A1	16	6	A2	QP(16,6,A2)	0.0412(2)		0.0485	−0.00560	0.0402	−0.00445
2075.232256(64)	14	0	A1	15	0	A2	QP(15,0,A2)	0.0507(11)		0.0483	−0.00553	0.0403	−0.00437
2085.622543(31)	13	6	A1	14	6	A2	QP(14,6,A2)	0.0410(2)	−0.00435(25)	0.0520	−0.00544	0.0442	−0.00437
2092.900901(36)	12	0	A1	13	0	A2	QP(13,0,A2)	0.0515(6)		0.0520	−0.00537	0.0447	−0.00429
2093.278567(22)	12	3	A1	13	3	A2	QP(13,3,A2)	0.0462(5)	−0.00408(13)	0.0526	−0.00539	0.0452	−0.00432
2110.249293(29)	10	0	A1	11	0	A2	QP(11,0,A2)	0.0541(2)	−0.00561(24)	0.0556	−0.00519	0.0489	−0.00420
2110.620142(24)	10	3	A1	11	3	A2	QP(11,3,A2)	0.0549(2)	−0.00472(13)	0.0561	−0.00520	0.0493	−0.00422
2122.013406(49)	9	9	A1	10	9	A2	QP(10,9,A2)	0.0533(2)	−0.00629(10)	0.0502	−0.00604	0.0395	−0.00487
2127.283798(33)	8	0	A1	9	0	A2	QP(3,0,A2)	0.0567(2)	−0.00490(26)	0.0591	−0.00499	0.0529	−0.00409
2127.648094(25)	8	3	A1	9	3	A2	QP(3,3,A2)	0.0504(4)	−0.00367(3)	0.0593	−0.00501	0.0529	−0.00412
2128.734645(16)	8	6	A1	9	6	A2	QP(3,6,A2)	0.0508(3)	−0.00381(2)	0.0584	−0.00518	0.0509	−0.00427
2137.122066(18)	7	6	A1	8	6	A2	QP(2,6,A2)	0.0506(5)	−0.00573(11)	0.0582	−0.00526	0.0500	−0.00433
2144.006717(19)	6	0	A1	7	0	A2	QP(2,0,A2)	0.0580(3)		0.0621	−0.00479	0.0562	−0.00397
2144.364667(13)	6	3	A1	7	3	A2	QP(2,3,A2)	0.0568(2)	−0.00472(4)	0.0619	−0.00483	0.0556	−0.00400
2145.431852(22)	6	6	A1	7	6	A2	QP(2,6,A2)	0.0570(6)	−0.00638(14)	0.0555	−0.00555	0.0457	−0.00455
2160.416737(21)	4	0	A1	5	0	A2	QP(5,0,A2)	0.0615(4)	−0.00451(3)	0.0646	−0.00455	0.0587	−0.00378
2160.768578(19)	4	3	A1	5	3	A2	QP(5,3,A2)	0.0605(3)	−0.00517(2)	0.0632	−0.00476	0.0564	−0.00397
2168.852039(16)	3	3	A1	4	3	A2	QP(4,3,A2)	0.0597(3)	−0.00601(2)	0.0616	−0.00516	0.0535	−0.00434
2176.509329(15)	2	0	A1	3	0	A2	QP(3,0,A2)	0.0632(3)	−0.00496(2)	0.0662	−0.00437	0.0602	−0.00373
2192.277904(44)	0	0	A1	1	0	A2	QP(1,0,A2)	0.0632(10)	−0.00349(24)	0.0679	−0.00480	0.0621	−0.00411
2057.271421(28)	16	1	E	17	1	E	QP(17,1,E)	0.0491(12)		0.0445	−0.00570	0.0359	−0.00445
2057.401191(27)	16	2	E	17	2	E	QP(17,2,E)	0.0452(15)		0.0447	−0.00573	0.0361	−0.00448
2057.917765(29)	16	4	E	17	4	E	QP(17,4,E)	0.0455(15)		0.0455	−0.00573	0.0369	−0.00450
2058.303590(30)	16	5	E	17	5	E	QP(17,5,E)	0.0387(11)		0.0461	−0.00571	0.0375	−0.00449
2066.316533(24)	15	1	E	16	1	E	QP(16,1,E)	0.0505(11)		0.0464	−0.00562	0.0381	−0.00442
2066.445132(68)	15	2	E	16	2	E	QP(16,2,E)	0.0445(12)		0.0466	−0.00564	0.0383	−0.00444
2066.958689(67)	15	4	E	16	4	E	QP(16,4,E)	0.0479(11)		0.0474	−0.00564	0.0391	−0.00445
2067.342955(65)	15	5	E	16	5	E	QP(16,5,E)	0.0425(11)		0.0480	−0.00562	0.0396	−0.00445
2068.926816(24)	15	8	E	16	8	E	QP(16,8,E)	0.0391(23)		0.0494	−0.00558	0.0410	−0.00445
2075.274531(29)	14	1	E	15	1	E	QP(15,1,E)	0.0507(11)		0.0483	−0.00554	0.0404	−0.00438

Also included are two sets of calculated O_2-broadening coefficients and O_2-induced pressure-shift coefficients.

[a] The values in parentheses represent one standard deviation uncertainties in the measured quantities in units of the last quoted digit.

[b] cm^{-1}.

[c] $cm^{-1}\,atm^{-1}$ at 296 K.

[d] $cm^{-1}\,atm^{-1}$ at the temperature of the spectra (298 ± 2 K).

Table 2 (*continued*)

Position[a,b]	J'	K'	N'	J''	K''	N''	Assignment	Measured $\gamma(O_2)$[a,c]	Measured $\delta(O_2)$[a,d]	Calc. 1 $\gamma(O_2)$[c]	Calc. 1 $\delta(O_2)$[c]	Calc. 2 $\gamma(O_2)$[c]	Calc. 2 $\delta(O_2)$[c]
2075.402106(28)	14	2	E	15	2	E	QP(15,2,E)	0.0482(10)		0.0486	−0.00556	0.0406	−0.00440
2075.912813(30)	14	4	E	15	4	E	QP(15,4,E)	0.0459(11)		0.0493	−0.00555	0.0413	−0.00441
2076.294370(32)	14	5	E	15	5	E	QP(15,5,E)	0.0439(10)		0.0498	−0.00554	0.0418	−0.00441
2077.299080(40)	14	7	E	15	7	E	QP(15,7,E)	0.0401(3)		0.0507	−0.00551	0.0426	−0.00441
2077.890464(46)	14	8	E	15	8	E	QP(15,8,E)	0.0406(2)		0.0510	−0.00551	0.0428	−0.00443
2079.548910(68)	14	10	E	15	10	E	QP(15,10,E)	0.0450(3)		0.0508	−0.00559	0.0422	−0.00451
2084.149499(46)	13	1	E	14	1	E	QP(14,1,E)	0.0504(2)		0.0502	−0.00546	0.0426	−0.00435
2084.276576(47)	13	2	E	14	2	E	QP(14,2,E)	0.0486(2)	−0.00400(19)	0.0504	−0.00547	0.0428	−0.00436
2084.783276(52)	13	4	E	14	4	E	QP(14,4,E)	0.0476(2)		0.0512	−0.00546	0.0435	−0.00437
2085.161893(50)	13	5	E	14	5	E	QP(14,5,E)	0.0427(2)		0.0516	−0.00545	0.0439	−0.00436
2086.161478(65)	13	7	E	14	7	E	QP(14,7,E)	0.0424(3)		0.0524	−0.00544	0.0445	−0.00438
2086.761088(20)	13	8	E	14	8	E	QP(14,8,E)	0.0411(11)	−0.00574(17)	0.0525	−0.00546	0.0445	−0.00441
2088.36703(133)	13	10	E	14	10	E	QP(14,10,E)	0.0463(2)		0.0517	−0.00561	0.0430	−0.00454
2089.216118(25)	13	11	E	14	11	E	QP(14,11,E)	0.0377(12)		0.0504	−0.00577	0.0412	−0.00467
2092.942869(35)	12	1	E	13	1	E	QP(13,1,E)	0.0509(11)	−0.00389(3)	0.0521	−0.00538	0.0448	−0.00431
2093.068939(36)	12	2	E	13	2	E	QP(13,2,E)	0.0505(10)	−0.00429(25)	0.0523	−0.00538	0.0449	−0.00431
2093.571535(40)	12	4	E	13	4	E	QP(13,4,E)	0.0505(6)		0.0530	−0.00537	0.0455	−0.00432
2093.947089(44)	12	5	E	13	5	E	QP(13,5,E)	0.0449(6)	−0.00536(28)	0.0534	−0.00536	0.0459	−0.00432
2094.940227(53)	12	7	E	13	7	E	QP(13,7,E)	0.0437(2)		0.0539	−0.00537	0.0462	−0.00435
2095.543217(68)	12	8	E	13	8	E	QP(13,8,E)	0.0424(10)	−0.00575(39)	0.0538	−0.00542	0.0458	−0.00440
2097.102367(21)	12	10	E	13	10	E	QP(13,10,E)	0.0471(11)	−0.00462(16)	0.0520	−0.00565	0.0431	−0.00460
2101.656260(28)	11	1	E	12	1	E	QP(12,1,E)	0.0498(2)	−0.00298(6)	0.0539	−0.00529	0.0469	−0.00426
2101.781140(28)	11	2	E	12	2	E	QP(12,2,E)	0.0510(2)	−0.00498(18)	0.0541	−0.00529	0.0471	−0.00427
2102.279414(31)	11	4	E	12	4	E	QP(12,4,E)	0.0506(2)	−0.00357(27)	0.0547	−0.00528	0.0476	−0.00428
2102.651791(35)	11	5	E	12	5	E	QP(12,5,E)	0.0496(3)	−0.00486(23)	0.0550	−0.00528	0.0478	−0.00428
2103.637379(36)	11	7	E	12	7	E	QP(12,7,E)	0.0447(6)		0.0552	−0.00532	0.0476	−0.00434
2104.240823(47)	11	8	E	12	8	E	QP(12,8,E)	0.0449(2)	−0.00567(17)	0.0548	−0.00539	0.0468	−0.00441
2105.758547(30)	11	10	E	12	10	E	QP(12,10,E)	0.0475(2)		0.0515	−0.00583	0.0419	−0.00474
2106.589394(28)	11	11	E	12	11	E	QP(12,11,E)	0.0554(19)		0.0468	−0.00633	0.0359	−0.00507
2110.290471(23)	10	1	E	11	1	E	QP(11,1,E)	0.0508(6)	−0.00368(2)	0.0557	−0.00519	0.0490	−0.00421
2110.414303(29)	10	2	E	11	2	E	QP(11,2,E)	0.0548(6)	−0.00466(18)	0.0558	−0.00520	0.0491	−0.00422
2110.908073(25)	10	4	E	11	4	E	QP(11,4,E)	0.0513(6)	−0.00385(15)	0.0564	−0.00519	0.0495	−0.00423
2111.277110(34)	10	5	E	11	5	E	QP(11,5,E)	0.0485(2)	−0.00425(17)	0.0566	−0.00520	0.0495	−0.00424
2112.254777(32)	10	7	E	11	7	E	QP(11,7,E)	0.0473(2)	−0.00437(28)	0.0563	−0.00529	0.0486	−0.00434
2112.856970(42)	10	8	E	11	8	E	QP(11,8,E)	0.0475(6)	−0.00475(36)	0.0553	−0.00543	0.0470	−0.00445
2114.336012(22)	10	10	E	11	10	E	QP(11,10,E)	0.0467(12)		0.0485	−0.00619	0.0377	−0.00498
2118.846389(56)	9	1	E	10	1	E	QP(10,1,E)	0.0528(2)	−0.00473(6)	0.0574	−0.00509	0.0510	−0.00416
2118.969088(22)	9	2	E	10	2	E	QP(10,2,E)	0.0545(2)	−0.00593(18)	0.0575	−0.00510	0.0511	−0.00416
2119.458304(63)	9	4	E	10	4	E	QP(10,4,E)	0.0527(2)		0.0579	−0.00510	0.0512	−0.00418
2119.824102(20)	9	5	E	10	5	E	QP(10,5,E)	0.0528(2)		0.0580	−0.00512	0.0511	−0.00421
2120.793542(26)	9	7	E	10	7	E	QP(10,7,E)	0.0503(2)	−0.00548(18)	0.0568	−0.00531	0.0489	−0.00436
2121.393184(39)	9	8	E	10	8	E	QP(10,8,E)	0.0505(6)	−0.00598(28)	0.0549	−0.00555	0.0459	−0.00455
2127.324235(33)	8	1	E	9	1	E	QP(3,1,E)	0.0553(2)	−0.00388(6)	0.0591	−0.00500	0.0529	−0.00410
2127.445865(33)	8	2	E	9	2	E	QP(3,2,E)	0.0571(2)	−0.00497(18)	0.0592	−0.00500	0.0529	−0.00411
2127.930811(17)	8	4	E	9	4	E	QP(3,4,E)	0.0559(4)	−0.00427(3)	0.0594	−0.00502	0.0527	−0.00414
2128.293139(20)	8	5	E	9	5	E	QP(3,5,E)	0.0509(4)	−0.00407(10)	0.0592	−0.00507	0.0522	−0.00418
2129.254141(33)	8	7	E	9	7	E	QP(3,7,E)	0.0504(3)	−0.00628(22)	0.0565	−0.00541	0.0479	−0.00444
2129.850280(60)	8	8	E	9	8	E	QP(3,8,E)	0.0508(10)	−0.00675(13)	0.0520	−0.00588	0.0415	−0.00476
2135.724287(25)	7	1	E	8	1	E	QP(2,1,E)	0.0568(5)	−0.00533(10)	0.0607	−0.00490	0.0546	−0.00404
2135.844846(17)	7	2	E	8	2	E	QP(2,2,E)	0.0589(2)	−0.00496(2)	0.0607	−0.00491	0.0546	−0.00405
2136.325393(18)	7	4	E	8	4	E	QP(2,4,E)	0.0573(5)	−0.00488(12)	0.0606	−0.00495	0.0539	−0.00409
2136.684507(23)	7	5	E	8	5	E	QP(2,5,E)	0.0548(2)	−0.00517(24)	0.0599	−0.00505	0.0528	−0.00417
2137.637081(49)	7	7	E	8	7	E	QP(2,7,E)	0.0548(2)	−0.00573(32)	0.0537	−0.00572	0.0435	−0.00466
2144.046517(17)	6	1	E	7	1	E	QP(2,1,E)	0.0590(3)	−0.00497(2)	0.0621	−0.00480	0.0562	−0.00398
2144.165974(17)	6	2	E	7	2	E	QP(2,2,E)	0.0602(3)	−0.00603(2)	0.0621	−0.00481	0.0560	−0.00398
2144.642158(22)	6	4	E	7	4	E	QP(2,4,E)	0.0582(4)	−0.00519(10)	0.0614	−0.00491	0.0546	−0.00406
2144.998223(24)	6	5	E	7	5	E	QP(2,5,E)	0.0565(6)	−0.00457(14)	0.0598	−0.00510	0.0521	−0.00422
2152.290508(20)	5	1	E	6	1	E	QP(6,1,E)	0.0613(4)	−0.00471(13)	0.0634	−0.00469	0.0575	−0.00389
2152.408893(19)	5	2	E	6	2	E	QP(6,2,E)	0.0604(3)	−0.00531(2)	0.0633	−0.00470	0.0572	−0.00390
2152.881090(25)	5	4	E	6	4	E	QP(6,4,E)	0.0591(6)	−0.00568(13)	0.0615	−0.00493	0.0542	−0.00409
2153.233942(37)	5	5	E	6	5	E	QP(6,5,E)	0.0573(11)	−0.00630(26)	0.0574	−0.00540	0.0481	−0.00446
2160.455854(22)	4	1	E	5	1	E	QP(5,1,E)	0.0620(5)	−0.00432(2)	0.0645	−0.00456	0.0585	−0.00379
2161.041472(36)	4	4	E	5	4	E	QP(5,4,E)	0.0575(10)	−0.00662(24)	0.0594	−0.00527	0.0506	−0.00439
2168.541880(16)	3	1	E	4	1	E	QP(4,1,E)	0.0625(3)	−0.00417(2)	0.0654	−0.00443	0.0593	−0.00372

(*continued on next page*)

Table 2 (*continued*)

Position[a,b]	J'	K'	N'	J''	K''	N''	Assignment	Measured $\gamma(O_2)$[a,c]	Measured $\delta(O_2)$[a,d]	Calc. 1 $\gamma(O_2)$[c]	Calc. 1 $\delta(O_2)$[c]	Calc. 2 $\gamma(O_2)$[c]	Calc. 2 $\delta(O_2)$[c]
2168.658320(17)	3	2	E	4	2	E	QP(4,2,E)	0.0620(4)	−0.00511(2)	0.0649	−0.00459	0.0584	−0.00387
2176.547906(16)	2	1	E	3	1	E	QP(3,1,E)	0.0630(4)	−0.00610(2)	0.0662	−0.00450	0.0600	−0.00385
2176.663425(18)	2	2	E	3	2	E	QP(3,2,E)	0.0629(4)	−0.00429(10)	0.0640	−0.00502	0.0567	−0.00427
2189.524699(23)	16	6	A2	16	6	A1	QQ(16,6,A1)	0.0392(16)		0.0464	−0.00553	0.0379	−0.00431
2193.022282(52)	15	9	A2	15	9	A1	QQ(15,9,A1)	0.0404(13)		0.0489	−0.00541	0.0404	−0.00426
2191.284302(29)	14	3	A2	14	3	A1	QQ(14,3,A1)	0.0489(15)		0.0492	−0.00541	0.0413	−0.00424
2196.531676(68)	14	12	A2	14	12	A1	QQ(14,12,A1)	0.0332(3)		0.0484	−0.00543	0.0387	−0.00430
2192.529204(36)	13	3	A2	13	3	A1	QQ(13,3,A1)	0.0464(21)		0.0510	−0.00532	0.0435	−0.00419
2195.626299(56)	13	9	A2	13	9	A1	QQ(13,9,A1)	0.0390(6)		0.0518	−0.00528	0.0435	−0.00419
2195.681065(27)	10	3	A2	10	3	A1	QQ(10,3,A1)	0.0449(10)		0.0564	−0.00500	0.0496	−0.00401
2196.713989(40)	10	6	A2	10	6	A1	QQ(10,6,A1)	0.0460(2)	−0.00441(18)	0.0562	−0.00502	0.0489	−0.00404
2196.544977(34)	9	3	A2	9	3	A1	QQ(3,3,A1)	0.0501(10)		0.0580	−0.00489	0.0514	−0.00395
2197.574336(23)	9	6	A2	9	6	A1	QQ(3,6,A1)	0.0502(2)		0.0573	−0.00495	0.0499	−0.00401
2197.318441(23)	8	3	A2	8	3	A1	QQ(2,3,A1)	0.0557(2)		0.0595	−0.00479	0.0530	−0.00389
2198.005949(27)	7	3	A2	7	3	A1	QQ(2,3,A1)	0.0574(6)		0.0608	−0.00469	0.0544	−0.00384
2199.025585(23)	7	6	A2	7	6	A1	QQ(2,6,A1)	0.0542(4)	−0.00523(2)	0.0575	−0.00492	0.0487	−0.00402
2199.109233(25)	5	3	A2	5	3	A1	QQ(5,3,A1)	0.0588(5)	−0.00334(10)	0.0625	−0.00457	0.0558	−0.00379
2195.230145(21)	15	12	A1	15	12	A2	QQ(15,12,A2)	0.0303(2)		0.0483	−0.00545	0.0390	−0.00429
2192.329063(47)	14	6	A1	14	6	A2	QQ(14,6,A2)	0.0417(14)		0.0500	−0.00535	0.0421	−0.00421
2197.729903(65)	13	12	A1	13	12	A2	QQ(13,12,A2)	0.0379(2)		0.0463	−0.00552	0.0357	−0.00435
2193.675761(40)	12	3	A1	12	3	A2	QQ(12,3,A2)	0.0470(12)		0.0529	−0.00522	0.0456	−0.00413
2194.715144(28)	12	6	A1	12	6	A2	QQ(12,6,A2)	0.0451(10)		0.0534	−0.00517	0.0458	−0.00411
2196.820297(68)	12	9	A1	12	9	A2	QQ(12,9,A2)	0.0404(2)	−0.00563(29)	0.0529	−0.00522	0.0445	−0.00417
2195.762621(27)	11	6	A1	11	6	A2	QQ(11,6,A2)	0.0449(5)		0.0549	−0.00508	0.0475	−0.00406
2198.016774(21)	11	9	A1	11	9	A2	QQ(11,9,A2)	0.0385(14)	−0.00502(16)	0.0534	−0.00519	0.0445	−0.00416
2198.184788(42)	10	9	A1	10	9	A2	QQ(10,9,A2)	0.0452(2)	−0.00534(24)	0.0521	−0.00523	0.0422	−0.00420
2199.205371(21)	9	9	A1	9	9	A2	QQ(3,9,A2)	0.0351(3)	−0.00548(6)	0.0409	−0.00567	0.0293	−0.00443
2198.344334(34)	8	6	A1	8	6	A2	QQ(2,6,A2)	0.0511(6)	−0.00462(12)	0.0580	−0.00491	0.0502	−0.00400
2198.599307(26)	6	3	A1	6	3	A2	QQ(6,3,A2)	0.0595(5)		0.0618	−0.00462	0.0554	−0.00380
2199.619251(19)	6	6	A1	6	6	A2	QQ(6,6,A2)	0.0471(3)	−0.00567(5)	0.0497	−0.00529	0.0383	−0.00425
2199.532830(27)	4	3	A1	4	3	A2	QQ(4,3,A2)	0.0607(6)		0.0626	−0.00456	0.0553	−0.00379
2199.871083(20)	3	3	A1	3	3	A2	QQ(3,3,A2)	0.0579(3)	−0.00619(6)	0.0592	−0.00478	0.0499	−0.00396
2189.627357(29)	15	1	E	15	1	E	QQ(15,1,E)	0.0473(14)		0.0467	−0.00553	0.0386	−0.00431
2191.474127(28)	15	7	E	15	7	E	QQ(15,7,E)	0.0429(16)		0.0486	−0.00542	0.0403	−0.00425
2193.571873(27)	15	10	E	15	10	E	QQ(15,10,E)	0.0464(11)	−0.00525(58)	0.0490	−0.00541	0.0403	−0.00426
2191.903781(64)	14	5	E	14	5	E	QQ(14,5,E)	0.0437(2)	−0.00489(20)	0.0498	−0.00537	0.0419	−0.00422
2193.359256(63)	14	8	E	14	8	E	QQ(14,8,E)	0.0396(3)		0.0504	−0.00533	0.0422	−0.00421
2194.885627(57)	14	10	E	14	10	E	QQ(14,10,E)	0.0450(11)		0.0503	−0.00536	0.0417	−0.00424
2198.463019(57)	14	14	E	14	14	E	QQ(14,14,E)	0.0153(5)	−0.00583(14)	0.0284	−0.00611	0.0186	−0.00462
2193.149030(28)	13	5	E	13	5	E	QQ(13,5,E)	0.0433(14)		0.0516	−0.00527	0.0439	−0.00416
2194.066362(39)	13	7	E	13	7	E	QQ(13,7,E)	0.0438(10)		0.0517	−0.00526	0.0440	−0.00416
2194.614319(31)	13	8	E	13	8	E	QQ(13,8,E)	0.0410(2)		0.0519	−0.00526	0.0439	−0.00418
2196.096733(50)	13	10	E	13	10	E	QQ(13,10,E)	0.0446(15)		0.0514	−0.0053	0.0426	−0.00421
2196.872813(25)	13	11	E	13	11	E	QQ(13,11,E)	0.0368(2)		0.0501	−0.00536	0.0407	−0.00425
2193.946147(59)	12	4	E	12	4	E	QQ(12,4,E)	0.0510(11)		0.0531	−0.00519	0.0458	−0.00412
2195.209446(24)	12	7	E	12	7	E	QQ(12,7,E)	0.0461(12)		0.0534	−0.00518	0.0457	−0.00412
2197.983464(59)	12	11	E	12	11	E	QQ(12,11,E)	0.0426(12)		0.0482	−0.00542	0.0378	−0.00430
2194.995425(32)	11	4	E	11	4	E	QQ(11,4,E)	0.0513(13)		0.0548	−0.00509	0.0477	−0.00406
2195.340838(68)	11	5	E	11	5	E	QQ(11,5,E)	0.0480(10)		0.0549	−0.00508	0.0477	−0.00406
2196.255476(24)	11	7	E	11	7	E	QQ(11,7,E)	0.0492(11)		0.0548	−0.00511	0.0471	−0.00409
2196.81344(188)	11	8	E	11	8	E	QQ(11,8,E)	0.0472(6)	−0.00526(35)	0.0544	−0.00514	0.0463	−0.00413
2198.224777(23)	11	10	E	11	10	E	QQ(11,10,E)	0.0452(10)		0.0502	−0.00533	0.0400	−0.00425
2195.488865(69)	10	2	E	10	2	E	QQ(10,2,E)	0.0522(23)		0.0562	−0.00502	0.0496	−0.00402
2196.294470(22)	10	5	E	10	5	E	QQ(10,5,E)	0.0485(10)	−0.00487(25)	0.0564	−0.00498	0.0493	−0.00401
2197.207058(25)	10	7	E	10	7	E	QQ(10,7,E)	0.0491(12)		0.0559	−0.00505	0.0481	−0.00407
2197.767814(23)	10	8	E	10	8	E	QQ(10,8,E)	0.0517(3)	−0.00474(21)	0.0550	−0.00509	0.0464	−0.00411
2199.148419(37)	10	10	E	10	10	E	QQ(10,10,E)	0.0298(6)	−0.00594(14)	0.0382	−0.00577	0.0268	−0.00448
2196.353169(29)	9	2	E	9	2	E	QQ(3,2,E)	0.0567(14)	−0.00422(24)	0.0579	−0.00491	0.0515	−0.00396
2197.156228(31)	9	5	E	9	5	E	QQ(3,5,E)	0.0499(10)		0.0577	−0.00491	0.0507	−0.00398
2198.065830(49)	9	7	E	9	7	E	QQ(3,7,E)	0.0501(6)		0.0565	−0.00500	0.0483	−0.00405
2197.585455(61)	8	4	E	8	4	E	QQ(2,4,E)	0.0572(12)		0.0592	−0.00480	0.0525	−0.00390
2197.927610(23)	8	5	E	8	5	E	QQ(2,5,E)	0.0527(2)		0.0588	−0.00485	0.0517	−0.00395
2199.396936(30)	8	8	E	8	8	E	QQ(2,8,E)	0.0392(5)	−0.00528(13)	0.0438	−0.00556	0.0321	−0.00438
2198.268009(50)	7	4	E	7	4	E	QQ(2,4,E)	0.0571(2)	−0.00438(35)	0.0603	−0.00474	0.0535	−0.00388

Table 2 (*continued*)

Position[a,b]	J'	K'	N'	J''	K''	N''	Assignment	Measured $\gamma(O_2)$[a,c]	Measured $\delta(O_2)$[a,d]	Calc. 1 $\gamma(O_2)$[c]	Calc. 1 $\delta(O_2)$[c]	Calc. 2 $\gamma(O_2)$[c]	Calc. 2 $\delta(O_2)$[c]
2199.514419(33)	7	7	E	7	7	E	QQ(2,7,E)	0.0413(5)	−0.00597(12)	0.0467	−0.00543	0.0350	−0.00432
2198.409825(66)	6	2	E	6	2	E	QQ(6,2,E)	0.0605(3)		0.0623	−0.00458	0.0562	−0.00377
2199.373855(32)	5	4	E	5	4	E	QQ(5,4,E)	0.0569(11)		0.0608	−0.00469	0.0531	−0.00388
2199.713118(24)	5	5	E	5	5	E	QQ(5,5,E)	0.0497(5)	−0.0059(10)	0.0527	−0.00515	0.0418	−0.00417
2199.22993(122)	4	1	E	4	1	E	QQ(4,1,E)	0.0623(3)	−0.0044(19)	0.0648	−0.00438	0.0588	−0.00366
2199.796912(26)	4	4	E	4	4	E	QQ(4,4,E)	0.0540(2)	−0.00676(17)	0.0559	−0.00498	0.0456	−0.00408
2199.568806(26)	3	1	E	3	1	E	QQ(3,1,E)	0.0636(3)	−0.00504(16)	0.0656	−0.00432	0.0595	−0.00364
2199.682353(36)	3	2	E	3	2	E	QQ(3,2,E)	0.0639(11)		0.0646	−0.00441	0.0578	−0.00370
2199.822449(68)	2	1	E	2	1	E	QQ(2,1,E)	0.0641(3)		0.0665	−0.00427	0.0603	−0.00361
2199.935655(27)	2	2	E	2	2	E	QQ(2,2,E)	0.0633(2)	−0.00569(16)	0.0628	−0.00454	0.0547	−0.00381
2199.990885(36)	1	1	E	1	1	E	QQ(1,1,E)	0.0628(11)		0.0667	−0.00428	0.0601	−0.00362
2317.474611(22)	17	0	A2	16	0	A1	QR(16,0,A1)	0.0462(19)		0.0444	−0.00560	0.0358	−0.00430
2311.767962(24)	16	3	A2	15	3	A1	QR(15,3,A1)	0.0441(15)		0.0470	−0.00551	0.0387	−0.00426
2305.287940(59)	15	0	A2	14	0	A1	QR(14,0,A1)	0.0482(3)		0.0483	−0.00540	0.0403	−0.00418
2305.603159(63)	15	3	A2	14	3	A1	QR(14,3,A1)	0.0471(3)		0.0489	−0.00540	0.0409	−0.00419
2302.163088(26)	14	9	A2	13	9	A1	QR(13,9,A1)	0.0418(10)		0.0523	−0.00507	0.0440	−0.00397
2292.605349(35)	13	0	A2	12	0	A1	QR(12,0,A1)	0.0508(10)	−0.00451(34)	0.0520	−0.00518	0.0447	−0.00404
2295.793318(60)	13	9	A2	12	9	A1	QR(12,9,A1)	0.0445(2)		0.0532	−0.00494	0.0449	−0.00388
2297.694008(22)	13	12	A2	12	12	A1	QR(12,12,A1)	0.0420(15)		0.0451	−0.00458	0.0342	−0.00355
2287.371684(18)	12	6	A2	11	6	A1	QR(11,6,A1)	0.0445(3)	−0.00515(2)	0.0552	−0.00495	0.0478	−0.00391
2289.343635(36)	12	9	A2	11	9	A1	QR(11,9,A1)	0.0473(3)	−0.00464(22)	0.0536	−0.00481	0.0451	−0.00379
2279.463090(22)	11	0	A2	10	0	A1	QR(10,0,A1)	0.0532(5)	−0.00523(16)	0.0556	−0.00494	0.0489	−0.00389
2279.786311(17)	11	3	A2	10	3	A1	QR(10,3,A1)	0.0469(3)	−0.00452(5)	0.0561	−0.00493	0.0493	−0.00389
2280.749089(17)	11	6	A2	10	6	A1	QR(10,6,A1)	0.0450(3)	−0.00475(6)	0.0566	−0.00482	0.0493	−0.00383
2282.879482(49)	11	9	A2	10	9	A1	QR(10,9,A1)	0.0495(2)		0.0532	−0.00470	0.0439	−0.00371
2273.053064(14)	10	3	A2	9	3	A1	QR(3,3,A1)	0.0476(2)	−0.00439(4)	0.0577	−0.00479	0.0511	−0.00381
2274.018788(17)	10	6	A2	9	6	A1	QR(3,6,A1)	0.0476(3)	−0.00456(6)	0.0577	−0.00470	0.0504	−0.00375
2275.377040(52)	10	9	A2	9	9	A1	QR(3,9,A1)	0.0533(2)	−0.00505(17)	0.0502	−0.00457	0.0395	−0.00362
2265.890204(23)	9	0	A2	8	0	A1	QR(2,0,A1)	0.0565(5)		0.0590	−0.00468	0.0528	−0.00373
2266.215339(18)	9	3	A2	8	3	A1	QR(2,3,A1)	0.0519(3)	−0.00461(5)	0.0593	−0.00466	0.0529	−0.00373
2267.184101(23)	9	6	A2	8	6	A1	QR(2,6,A1)	0.0501(4)	−0.00420(2)	0.0584	−0.00460	0.0508	−0.00369
2259.275598(21)	8	3	A2	7	3	A1	QR(2,3,A1)	0.0544(3)	−0.00392(5)	0.0607	−0.00454	0.0544	−0.00367
2260.247839(16)	8	6	A2	7	6	A1	QR(2,6,A1)	0.0517(3)	−0.00220(6)	0.0581	−0.00452	0.0500	−0.00366
2251.910436(18)	7	0	A2	6	0	A1	QR(6,0,A1)	0.0587(4)		0.0621	−0.00442	0.0562	−0.00359
2252.237768(15)	7	3	A2	6	3	A1	QR(6,3,A1)	0.0562(2)	−0.00439(4)	0.0619	−0.00443	0.0556	−0.00362
2245.103197(18)	6	3	A2	5	3	A1	QR(5,3,A1)	0.0580(3)		0.0628	−0.00436	0.0564	−0.00360
2237.543624(17)	5	0	A2	4	0	A1	QR(4,0,A1)	0.0606(3)		0.0646	−0.00424	0.0587	−0.00356
2230.551878(15)	4	3	A2	3	3	A1	QR(3,3,A1)	0.0595(3)	−0.00381(6)	0.0615	−0.00411	0.0534	−0.00337
2222.806647(17)	3	0	A2	2	0	A1	QR(2,0,A1)	0.0624(3)	−0.00413(2)	0.0662	−0.00418	0.0602	−0.00349
2207.713936(19)	1	0	A2	0	0	A1	QR(0,0,A1)	0.0619(4)	−0.00348(11)				
2317.796463(64)	17	3	A1	16	3	A2	QR(16,3,A2)	0.0439(5)		0.0450	−0.00561	0.0364	−0.00433
2311.446157(43)	16	0	A1	15	0	A2	QR(15,0,A2)	0.0481(10)		0.0463	−0.00550	0.0380	−0.00424
2312.703137(25)	16	6	A1	15	6	A2	QR(15,6,A2)	0.0401(11)		0.0485	−0.00542	0.0402	−0.00421
2305.610420(64)	15	3	A1	14	3	A2	QR(14,3,A2)	0.0471(3)		0.0489	−0.00540	0.0409	−0.00419
2306.553741(44)	15	6	A1	14	6	A2	QR(14,6,A2)	0.0420(5)	−0.00426(28)	0.0503	−0.00531	0.0422	−0.00414
2308.426857(38)	15	9	A1	14	9	A2	QR(14,9,A2)	0.0407(11)		0.0510	−0.00519	0.0427	−0.00405
2299.006220(55)	14	0	A1	13	0	A2	QR(13,0,A2)	0.0502(2)		0.0501	−0.00529	0.0425	−0.00411
2300.278391(43)	14	6	A1	13	6	A2	QR(13,6,A2)	0.0414(2)	−0.00381(28)	0.0520	−0.00519	0.0442	−0.00407
2293.882848(28)	13	6	A1	12	6	A2	QR(12,6,A2)	0.0420(5)	−0.00508(12)	0.0537	−0.00507	0.0461	−0.00399
2286.089687(21)	12	0	A1	11	0	A2	QR(11,0,A2)	0.0510(5)		0.0538	−0.00506	0.0468	−0.00397
2286.411976(15)	12	3	A1	11	3	A2	QR(11,3,A2)	0.0470(2)	−0.00413(5)	0.0543	−0.00506	0.0473	−0.00397
2272.728845(32)	10	0	A1	9	0	A2	QR(3,0,A2)	0.0551(6)	−0.00471(13)	0.0574	−0.00482	0.0509	−0.00381
2258.949873(25)	8	0	A1	7	0	A2	QR(2,0,A2)	0.0572(5)		0.0606	−0.00454	0.0546	−0.00365
2253.213008(25)	7	6	A1	6	6	A2	QR(6,6,A2)	0.0562(5)		0.0555	−0.00450	0.0457	−0.00364
2244.774237(24)	6	0	A1	5	0	A2	QR(5,0,A2)	0.0605(6)		0.0635	−0.00431	0.0576	−0.00356
2237.873579(15)	5	3	A1	4	3	A2	QR(4,3,A2)	0.0601(2)	−0.00344(5)	0.0632	−0.00429	0.0563	−0.00356
2230.220399(14)	4	0	A1	3	0	A2	QR(3,0,A2)	0.0616(3)	−0.00372(2)	0.0655	−0.00424	0.0595	−0.00358
2215.303911(15)	2	0	A1	1	0	A2	QR(1,0,A2)	0.0636(3)	−0.00421(2)	0.0667	−0.00383	0.0607	−0.00316
2317.511265(47)	17	1	E	16	1	E	QR(16,1,E)	0.0435(14)		0.0445	−0.00559	0.0359	−0.00430
2317.614817(26)	17	2	E	16	2	E	QR(16,2,E)	0.0445(15)		0.0447	−0.00561	0.0361	−0.00432
2311.481441(52)	16	1	E	15	1	E	QR(15,1,E)	0.0483(3)		0.0464	−0.00550	0.0381	−0.00424
2311.586983(54)	16	2	E	15	2	E	QR(15,2,E)	0.0437(10)	−0.00479(27)	0.0466	−0.00552	0.0383	−0.00426
2312.008722(69)	16	4	E	15	4	E	QR(15,4,E)	0.0436(11)		0.0474	−0.00549	0.0391	−0.00426
2312.321294(65)	16	5	E	15	5	E	QR(15,5,E)	0.0412(3)		0.0479	−0.00546	0.0396	−0.00424

(*continued on next page*)

Table 2 (*continued*)

Position[a,b]	J'	K'	N'	J''	K''	N''	Assignment	Measured $\gamma(O_2)$[a,c]	Measured $\delta(O_2)$[a,d]	Calc. 1 $\gamma(O_2)$[c]	Calc. 1 $\delta(O_2)$[c]	Calc. 2 $\gamma(O_2)$[c]	Calc. 2 $\delta(O_2)$[c]
2305.323400(58)	15	1	E	14	1	E	QR(14,1,E)	0.0495(3)	−0.00306(35)	0.0483	−0.00540	0.0404	−0.00419
2305.429766(58)	15	2	E	14	2	E	QR(14,2,E)	0.0470(2)		0.0485	−0.00541	0.0406	−0.00420
2305.853794(64)	15	4	E	14	4	E	QR(14,4,E)	0.0467(2)		0.0493	−0.00538	0.0413	−0.00419
2306.170222(69)	15	5	E	14	5	E	QR(14,5,E)	0.0436(3)		0.0498	−0.00535	0.0418	−0.00417
2306.997466(59)	15	7	E	14	7	E	QR(14,7,E)	0.0397(10)		0.0507	−0.00527	0.0426	−0.00411
2307.461114(62)	15	8	E	14	8	E	QR(14,8,E)	0.0408(10)		0.0510	−0.00523	0.0428	−0.00408
2299.041593(55)	14	1	E	13	1	E	QR(13,1,E)	0.0478(2)	−0.00288(11)	0.0502	−0.00530	0.0426	−0.00412
2299.148668(55)	14	2	E	13	2	E	QR(13,2,E)	0.0478(2)	−0.00507(16)	0.0504	−0.00530	0.0428	−0.00413
2299.574570(59)	14	4	E	13	4	E	QR(13,4,E)	0.0478(2)		0.0511	−0.00527	0.0434	−0.00412
2299.892520(64)	14	5	E	13	5	E	QR(13,5,E)	0.0454(2)	−0.00543(18)	0.0516	−0.00523	0.0439	−0.00409
2300.727737(64)	14	7	E	13	7	E	QR(13,7,E)	0.0416(3)		0.0523	−0.00515	0.0445	−0.00404
2301.212587(64)	14	8	E	13	8	E	QR(13,8,E)	0.0408(10)		0.0525	−0.00511	0.0445	−0.00401
2302.615635(26)	14	10	E	13	10	E	QR(13,10,E)	0.0451(10)		0.0516	−0.00502	0.0430	−0.00392
2292.640846(25)	13	1	E	12	1	E	QR(12,1,E)	0.0498(2)		0.0521	−0.00519	0.0448	−0.00405
2292.748233(34)	13	2	E	12	2	E	QR(12,2,E)	0.0492(2)	−0.00449(19)	0.0523	−0.00519	0.0449	−0.00405
2293.175796(37)	13	4	E	12	4	E	QR(12,4,E)	0.0499(11)	−0.00502(15)	0.0529	−0.00515	0.0455	−0.00404
2293.495027(39)	13	5	E	12	5	E	QR(12,5,E)	0.0450(3)	−0.00519(22)	0.0533	−0.00511	0.0459	−0.00401
2294.335716(51)	13	7	E	12	7	E	QR(12,7,E)	0.0431(5)	−0.00403(35)	0.0538	−0.00503	0.0462	−0.00396
2294.835552(59)	13	8	E	12	8	E	QR(12,8,E)	0.0419(2)		0.0537	−0.00499	0.0458	−0.00393
2296.201900(31)	13	10	E	12	10	E	QR(12,10,E)	0.0466(3)		0.0520	−0.00488	0.0431	−0.00381
2296.911132(37)	13	11	E	12	11	E	QR(12,11,E)	0.0471(15)		0.0498	−0.00480	0.0400	−0.00373
2286.125396(21)	12	1	E	11	1	E	QR(11,1,E)	0.0495(5)		0.0539	−0.00507	0.0469	−0.00397
2286.233041(21)	12	2	E	11	2	E	QR(11,2,E)	0.0502(4)	−0.00592(10)	0.0541	−0.00507	0.0470	−0.00398
2286.661957(22)	12	4	E	11	4	E	QR(11,4,E)	0.0509(5)	−0.00474(11)	0.0547	−0.00502	0.0475	−0.00396
2286.982251(30)	12	5	E	11	5	E	QR(11,5,E)	0.0482(5)	−0.00256(13)	0.0550	−0.00499	0.0478	−0.00393
2287.827389(31)	12	7	E	11	7	E	QR(11,7,E)	0.0441(2)	−0.00489(17)	0.0552	−0.00491	0.0476	−0.00388
2288.337913(38)	12	8	E	11	8	E	QR(11,8,E)	0.0442(3)		0.0547	−0.00486	0.0468	−0.00384
2289.674483(26)	12	10	E	11	10	E	QR(11,10,E)	0.0461(11)		0.0515	−0.00475	0.0419	−0.00372
2290.384503(20)	12	11	E	11	11	E	QR(11,11,E)	0.0512(17)		0.0468	−0.00458	0.0359	−0.00358
2279.498974(22)	11	1	E	10	1	E	QR(10,1,E)	0.0513(5)	−0.00458(12)	0.0557	−0.00495	0.0490	−0.00389
2279.607018(22)	11	2	E	10	2	E	QR(10,2,E)	0.0533(4)	−0.00494(10)	0.0558	−0.00494	0.0491	−0.00390
2280.037032(20)	11	4	E	10	4	E	QR(10,4,E)	0.0515(4)	−0.00469(3)	0.0563	−0.00489	0.0494	−0.00387
2280.358249(22)	11	5	E	10	5	E	QR(10,5,E)	0.0488(4)	−0.00360(10)	0.0566	−0.00486	0.0495	−0.00385
2281.207271(29)	11	7	E	10	7	E	QR(10,7,E)	0.0463(6)	−0.00363(15)	0.0562	−0.00479	0.0486	−0.00380
2281.725124(36)	11	8	E	10	8	E	QR(10,8,E)	0.0469(10)	−0.00469(33)	0.0552	−0.00475	0.0470	−0.00376
2283.036919(39)	11	10	E	10	10	E	QR(10,10,E)	0.0459(11)		0.0485	−0.00458	0.0377	−0.00360
2272.764956(19)	10	1	E	9	1	E	QR(3,1,E)	0.0514(4)	−0.00309(2)	0.0574	−0.00482	0.0510	−0.00381
2272.873107(18)	10	2	E	9	2	E	QR(3,2,E)	0.0536(3)	−0.00516(2)	0.0575	−0.00481	0.0510	−0.00381
2273.304464(20)	10	4	E	9	4	E	QR(3,4,E)	0.0540(3)	−0.00457(2)	0.0579	−0.00476	0.0512	−0.00379
2273.626528(21)	10	5	E	9	5	E	QR(3,5,E)	0.0500(4)	−0.00426(3)	0.0580	−0.00473	0.0510	−0.00377
2274.479019(29)	10	7	E	9	7	E	QR(3,7,E)	0.0496(6)	−0.00288(21)	0.0568	−0.00467	0.0489	−0.00373
2275.002737(42)	10	8	E	9	8	E	QR(3,8,E)	0.0503(11)		0.0548	−0.00464	0.0459	−0.00370
2265.926421(23)	9	1	E	8	1	E	QR(2,1,E)	0.0547(5)	−0.00421(10)	0.0591	−0.00469	0.0529	−0.00373
2266.034879(23)	9	2	E	8	2	E	QR(2,2,E)	0.0556(4)	−0.00537(3)	0.0592	−0.00468	0.0529	−0.00373
2266.467519(25)	9	4	E	8	4	E	QR(2,4,E)	0.0540(4)	−0.00505(10)	0.0593	−0.00464	0.0527	−0.00372
2266.790672(27)	9	5	E	8	5	E	QR(2,5,E)	0.0523(5)	−0.00441(12)	0.0591	−0.00462	0.0522	−0.00371
2267.646317(42)	9	7	E	8	7	E	QR(2,7,E)	0.0493(11)		0.0565	−0.00458	0.0479	−0.00368
2268.174403(65)	9	8	E	8	8	E	QR(2,8,E)	0.0502(3)	−0.00429(48)	0.0519	−0.00456	0.0415	−0.00364
2258.986148(25)	8	1	E	7	1	E	QR(2,1,E)	0.0562(5)	−0.00416(14)	0.0606	−0.00455	0.0546	−0.00366
2259.094979(24)	8	2	E	7	2	E	QR(2,2,E)	0.0580(4)	−0.00560(3)	0.0607	−0.00455	0.0545	−0.00366
2259.528898(28)	8	4	E	7	4	E	QR(2,4,E)	0.0569(6)	−0.00437(13)	0.0605	−0.00452	0.0539	−0.00366
2259.853157(32)	8	5	E	7	5	E	QR(2,5,E)	0.0545(2)	−0.00351(25)	0.0599	−0.00452	0.0527	−0.00366
2260.712030(35)	8	7	E	7	7	E	QR(2,7,E)	0.0536(10)	−0.00357(33)	0.0537	−0.00454	0.0435	−0.00365
2251.946879(19)	7	1	E	6	1	E	QR(6,1,E)	0.0590(4)	−0.00415(2)	0.0621	−0.00442	0.0562	−0.00360
2252.056106(18)	7	2	E	6	2	E	QR(6,2,E)	0.0587(3)	−0.00466(6)	0.0621	−0.00443	0.0560	−0.00361
2252.491577(21)	7	4	E	6	4	E	QR(6,4,E)	0.0588(4)	−0.00469(10)	0.0614	−0.00444	0.0546	−0.00363
2252.816845(25)	7	5	E	6	5	E	QR(6,5,E)	0.0583(5)	−0.00299(12)	0.0598	−0.00445	0.0521	−0.00363
2244.810856(24)	6	1	E	5	1	E	QR(5,1,E)	0.0618(5)	−0.00298(14)	0.0634	−0.00432	0.0575	−0.00357
2244.920343(24)	6	2	E	5	2	E	QR(5,2,E)	0.0596(4)	−0.00483(2)	0.0633	−0.00435	0.0572	−0.00359
2245.357698(34)	6	4	E	5	4	E	QR(5,4,E)	0.0596(6)	−0.00394(15)	0.0615	−0.00437	0.0542	−0.00360
2245.684130(47)	6	5	E	5	5	E	QR(5,5,E)	0.0602(12)		0.0574	−0.00442	0.0481	−0.00360
2237.580368(18)	5	1	E	4	1	E	QR(4,1,E)	0.0603(4)	−0.00201(3)	0.0645	−0.00427	0.0585	−0.00358
2237.690441(18)	5	2	E	4	2	E	QR(4,2,E)	0.0606(3)	−0.00332(6)	0.0642	−0.00430	0.0580	−0.00359
2238.129428(27)	5	4	E	4	4	E	QR(4,4,E)	0.0591(6)	−0.00338(15)	0.0593	−0.00430	0.0506	−0.00351

Table 2 (*continued*)

Position[a,b]	J'	K'	N'	J''	K''	N''	Assignment	Measured $\gamma(O_2)$[a,c]	Measured $\delta(O_2)$[a,d]	Calc. 1 $\gamma(O_2)$[c]	Calc. 1 $\delta(O_2)$[c]	Calc. 2 $\gamma(O_2)$[c]	Calc. 2 $\delta(O_2)$[c]
2230.257360(15)	4	1	E	3	1	E	QR(3,1,E)	0.0608(3)	−0.00173(2)	0.0654	−0.00425	0.0593	−0.00358
2230.367915(15)	4	2	E	3	2	E	QR(3,2,E)	0.0611(3)	−0.00449(6)	0.0648	−0.00420	0.0584	−0.00350
2222.843784(18)	3	1	E	2	1	E	QR(2,1,E)	0.0611(4)		0.0662	−0.00408	0.0600	−0.00340
2222.954834(20)	3	2	E	2	2	E	QR(2,2,E)	0.0620(4)	−0.00412(10)	0.0640	−0.00389	0.0566	−0.00321
2215.341169(17)	2	1	E	1	1	E	QR(1,1,E)	0.0619(4)	−0.00265(12)	0.0663	−0.00371	0.0598	−0.00307

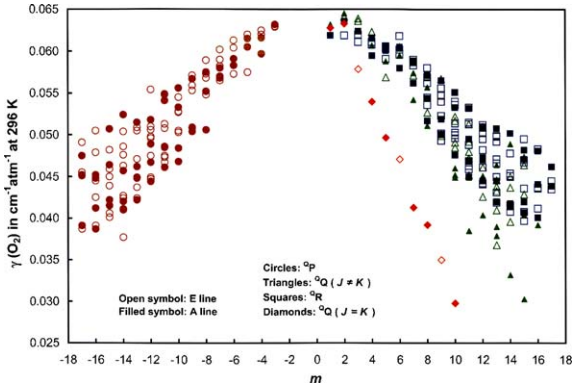

Fig. 2. Measured O_2-broadening coefficients, $\gamma(O_2)$, ($cm^{-1}\,atm^{-1}$ at 296 K) in the ^{O}P-, ^{O}Q-, and ^{O}R-branches as a function of m. The $J'' = K$ transitions in the ^{O}Q-branch are plotted with diamond symbols highlighting the rapidly falling trend of the corresponding O_2-broadening coefficients with m.

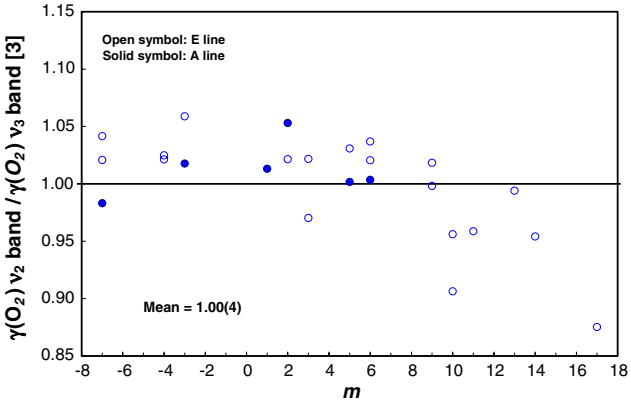

Fig. 3. Comparisons between the O_2-broadening coefficients obtained in the present study and those reported in [3].

3.2. Discussion of the measured O_2-induced pressure-shift coefficients

The measured O_2-induced pressure-shift coefficients have been plotted as a function of m in Fig. 4. All of our measured pressure-induced O_2-shift coefficients, $\delta(O_2)$, in Table 2 are between −0.0017 and −0.0068 $cm^{-1}\,atm^{-1}$ at the temperature of the spectra. The O_2-induced pressure-shift coefficients for ^{Q}Q-branch $J'' = K$ transitions are smaller than shifts with the same m value but different K values. Their trend with m is not as clearly defined as for the corresponding O_2-broadening coefficients presented in Fig. 2.

4. Theoretical modelling of broadening and shift coefficients

4.1. General formulation

Assuming that CH_3D behaves like a linear molecule for its interaction with O_2, we have used the semi-classical model of Robert and Bonamy [9]. Indeed, the three H atoms are considered as a single atom (denoted $_3H$) situated at the position of their projection on the C–D axis. The total intermolecular potential V_T involves in addition to the electrostatic interactions V_e, the atom–atom Lennard-Jones (LJ) model V_{aa} such that

$$V_T = V_{\Omega_1 Q_2} + V_{\Omega_1 \Phi_2} + V_{\Phi_1 Q_2} + V_{\Phi_1 \Phi_2} + \sum_{i,j} 4\varepsilon_{ij}\left[\left(\frac{\sigma_{ij}}{r_{ij}}\right)^{12} - \left(\frac{\sigma_{ij}}{r_{ij}}\right)^{6}\right], \quad (3)$$

where the index 1 refers to the absorber (CH_3D) and the index 2 to the perturber (O_2); Q, Ω, and Φ are the quadrupole, octopole, and molecular hexadecapole moments (note that we have neglected the very weak dipole and quadrupole moments of CH_3D); ε_{ij} and σ_{ij} are the LJ parameters for the interaction of the ith atom for molecule 1 ($_3H$, C, and D) and jth atom for molecule 2, and r_{ij} is the distance between these atoms. By expanding r_{ij} in power series of the intermolecular distance r, V_T can be expressed in terms of the spherical harmonics considered for each molecule and the intramolecular distances r_{1i} of $_3H{\equiv}C$–D and r_{2j} of O–O of each atom i or j to their mass center. The equivalent straight-path trajectory used [12] includes the influence of the isotropic potential taken as the spherical average $u_{000}(r)$ of V_{aa} which is well fitted by a LJ (14.2-6.1) potential. Note that the vibrational dephasing contribution to the line shifts was calculated as in [2] using a LJ (14-6) potential.

The LJ parameters $_3H$–$_3H$, C–C, and D–D for $_3HCD$–$_3HCD$ interactions were evaluated previously [1]. For O_2, we have considered the exact LJ parameters derived from experimental values of second virial coefficients $B(T)$ in the temperature range 200–400 K [13]. The parameters $_3H$–O, C–O, and D–O for $_3HCD$–O_2 interactions are obtained using the usual mixing rules $\sigma_{ij} = (\sigma_{ii} + \sigma_{jj})/2$ and $\varepsilon_{ij} = (\varepsilon_{ii}\ \varepsilon_{jj})^{1/2}$. The rotational constants B and D used for the ν_2 band of CH_3D were evaluated previously [1]. We assumed the ground vibrational state for the perturber during the collisions and we used the rotational constants B_0 and D_0 of O_2 given in [14]. The electric multipole moments and the LJ molecular

Table 3
Coefficients for the empirical expansions of the O_2-broadening parameters in the v_2 band

All ^QP and ^QR transitions, and ^QQ transitions with $J'' \neq K$		^QQ transitions with $J'' = K$	^{Q}Q transitions with $J'' = K+1$
Band	v_2	v_2	v_2
c_0	0.0613(3)	0.0624(2)	0.0651(6)
c_1	$-6.18(21)\times10^{-5}$	$-3.90(20)\times10^{-4}$	$-2.13(31)\times10^{-4}$
c_2	$-7.72(52)\times10^{-5}$	$7.95(36)\times10^{-7}$	$3.90(35)\times10^{-7}$
RMS error	4.02	1.52	1.39
No. of lines	300	11	9

The values in parentheses represent one standard deviation uncertainties in the measured quantities in units of the last quoted digit.

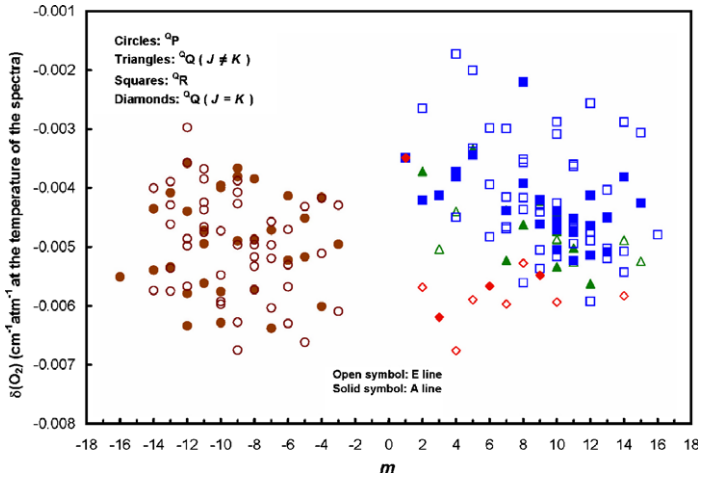

Fig. 4. Measured O_2-induced pressure-shift coefficients, $\delta(O_2)$, (cm^{-1} atm^{-1} at the temperature of the spectra) as a function of m.

parameters ε and σ used for CH_3D and O_2 are given in Table 4. The atom–atom LJ parameters ε_{ii}, σ_{ii}, ε_{jj} σ_{jj}, the intramolecular distances r_{1i} of CH_3D and r_{2j} of O_2, and the LJ parameters ε_u, σ_u, m, and n fitting $u_{000}(r)$ are given in Table 5. We have only considered the transitions induced by collisions with $\Delta K = 0$ for CH_3D associated with the usual selection rules for the absorber and perturber molecules, $\Delta J = 0, \pm1$ for a dipolar transition up to $\Delta J = 0$, ±1, ±2, ±3, ±4 for a hexadecapolar transition.

In a first calculation (calc. 1), similar to that carried out for CH_3D–N_2 [2], we used for the isotropic potential governing the trajectory model a LJ (m–n) potential fitting $u_{000}(r)$ (Table 5). As the results of this calculation are generally overestimated and are significantly dependent on the isotropic potential, in a second calculation (calc. 2) we considered a LJ (12-6) potential with parameters ε and σ determined from the usual combination rules of molecular parameters for the absorber and the perturber (Table 4).

Table 4
Molecular parameters for CH_3D and O_2 used in the calculations

Molecule	Q (D Å)	Ω (D Å^2)	Φ (D Å^3)	ε (K)	σ (Å)
CH_3D	0	3.10[b]	6.55[b]	130.65[c]	3.897[c]
O_2	0.40[a]	0	4.3[a]	117.69[d]	3.507[d]

[a] Ref. [15].
[b] Ref. [3].
[c] Ref. [16].
[d] Ref. [6].

4.2. Broadening coefficients and comparison with experimental data

The O_2-broadening coefficients were computed for lines at $T = 296$ K in the ^QP-, ^QQ-, and ^QR-branches of the v_2 band, by including the contributions from O_2 in

Table 5
Atom–atom LJ parameters ε_{ii}, ε_{jj}, σ_{ii}, σ_{jj}, intramolecular distances r_{1i} of $_3$HCD, r_{2j} of O_2 and LJ (m–n) parameters ε_u, σ_u fitting $u_{000}(r)$ for $_3$HCD–O_2 interactions

ε_{ii}, ε_{jj} (K)	σ_{ii}, σ_{jj} (Å)	r_{1i}, r_{2j} (Å)	ε_u (K)	σ_u (Å)	m	n
$\varepsilon_{C-C} = 61.365$	$\sigma_{C-C} = 3.141$	$\lvert r_{1C}\rvert = 0.0638$	109.064	3.5972	14.2	6.1
$\varepsilon_3H{-}_3H = 14.706$	$\sigma_3H{-}_3H = 3.845$	$\lvert r_{1_3H}\rvert = 0.4313$				
$\varepsilon_{D-D} = 13.232$	$\sigma_{D-D} = 2.662$	$\lvert r_{1D}\rvert = 1.0279$				
$\varepsilon_{O-O} = 51.8037$	$\sigma_{O-O} = 3.0058$	$\lvert r_{2O}\rvert = 0.605$				

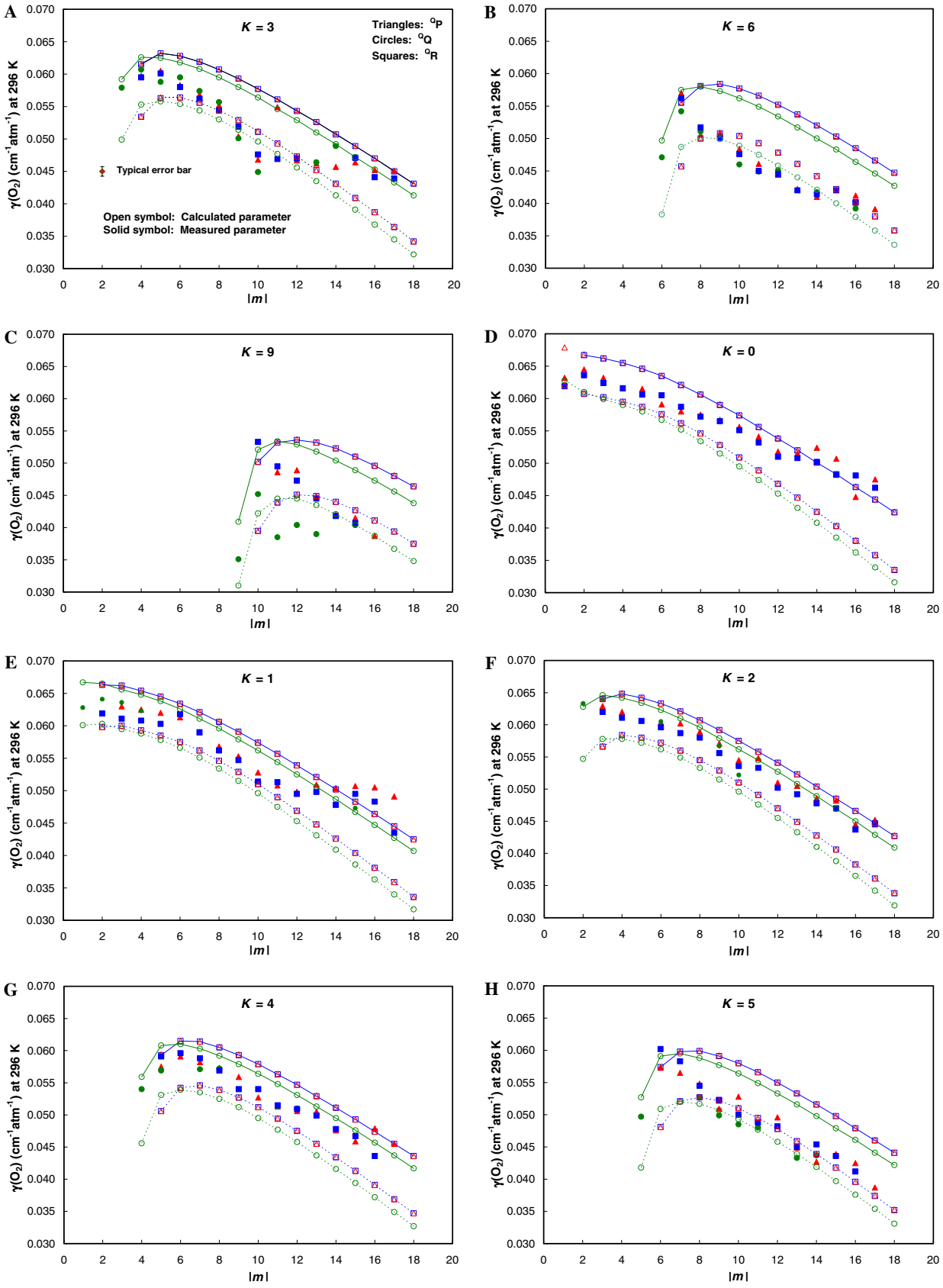

Fig. 5. Variation of measured, empirically derived, and theoretically calculated O_2-broadening coefficients with $|m|$ for (A) $K = 3$; (B) $K = 6$; (C) $K = 9$; (D) $K = 0$; (E) $K = 1$; (F) $K = 2$; (G) $K = 4$; and (H) $K = 5$. For a given $|m|$, the theoretical broadening coefficients for the ^{O}P and ^{O}R lines are very nearly the same. The broadening coefficients connected with smooth line are obtained using calculation 1 and those connected with dotted line are obtained using calculation 2.

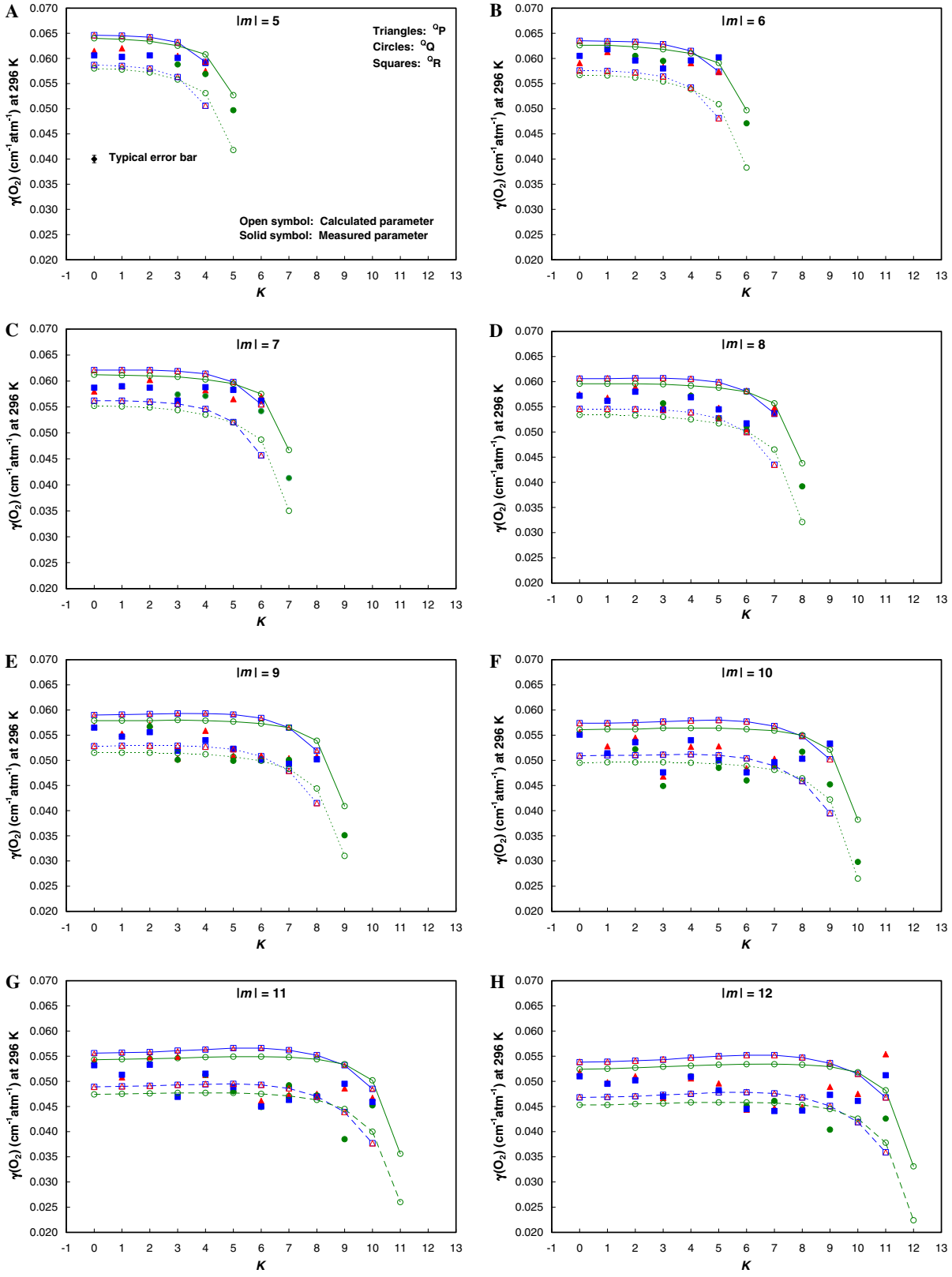

Fig. 6. Variation of measured, empirically derived, and theoretically calculated O_2-broadening coefficients $\gamma(O_2)$ versus K in select $|m|$ series ($|m| = 5$–12) in the ${}^{Q}P$-, ${}^{Q}Q$-, and ${}^{Q}R$-branches. The broadening coefficients connected with smooth line are obtained using calculation 1 and those connected with dotted line are obtained using calculation 2.

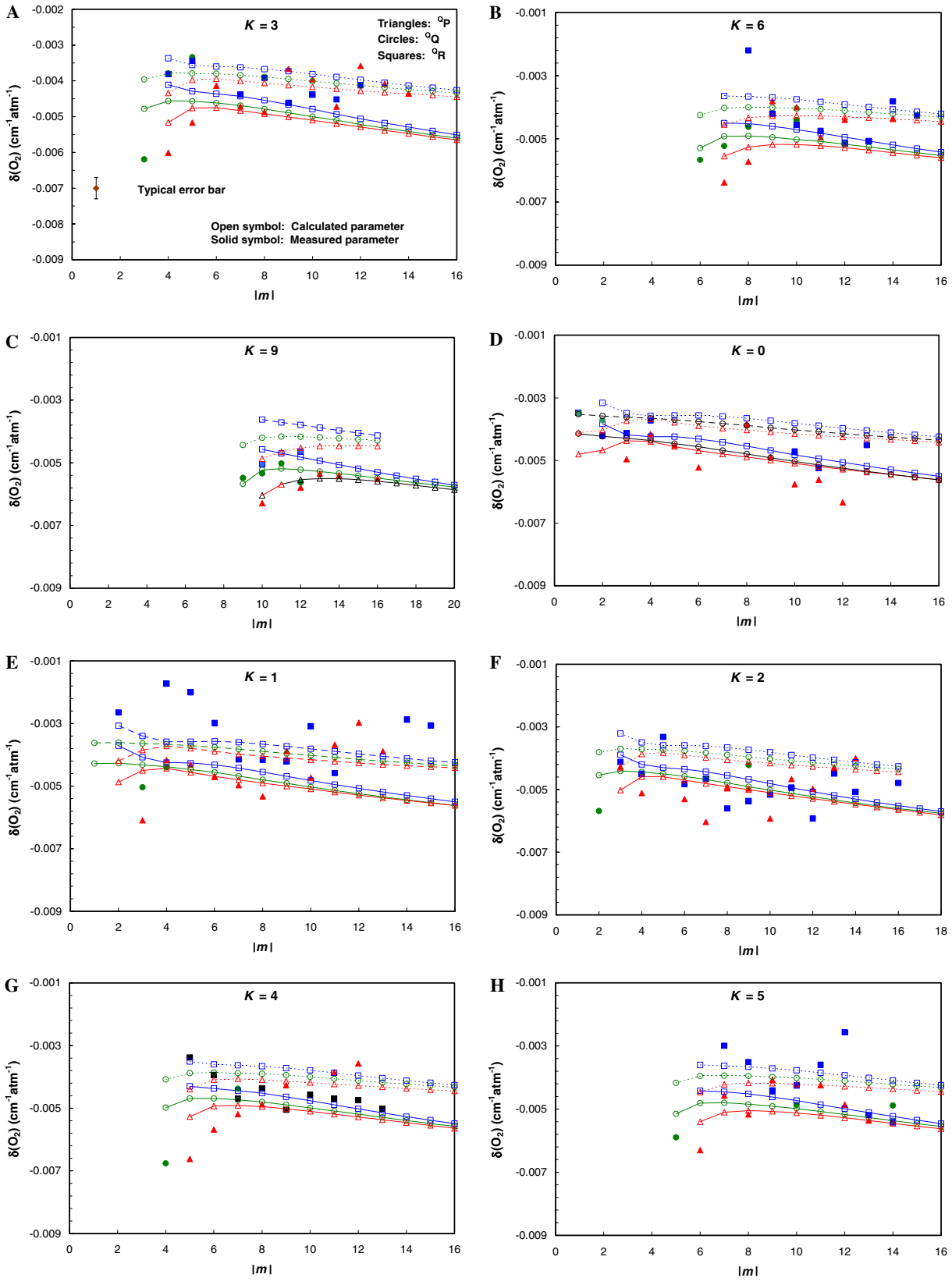

Fig. 7. Measured and theoretical O_2-induced pressure-shift coefficients, $\delta(O_2)$ as a function of $|m|$ for selected K series transitions: (A) $K = 3$, (B) $K = 6$, (C) $K = 9$, (D) $K = 0$, (E) $K = 1$, (F) $K = 2$, (G) $K = 4$, and (H) $K = 5$. The pressure-shift coefficients connected with smooth line are obtained using calculation 1 and those connected with dotted line are obtained using calculation 2.

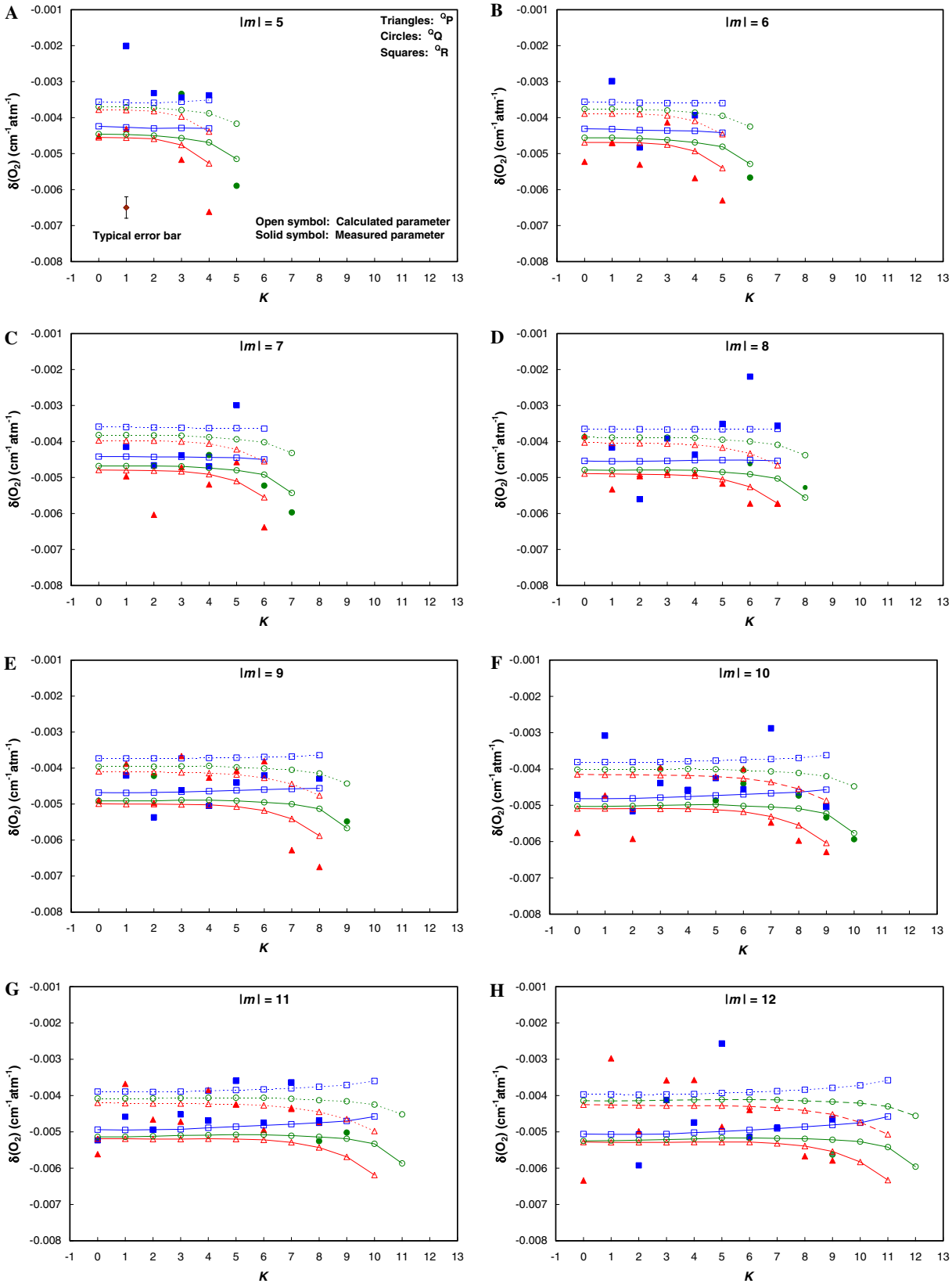

Fig. 8. Theoretically calculated and measured O_2-shift coefficients, $\delta(O_2)$, as a function of K for (A) $|m| = 5$, (B) $|m| = 6$, (C) $|m| = 7$, (D) $|m| = 8$, (E) $|m| = 9$, (F) $|m| = 10$, (G) $|m| = 11$, and (H) $|m| = 12$. The pressure-shift coefficients connected with smooth line are obtained using calculation 1 and those connected with dotted line are obtained using calculation 2.

the fundamental state with J_2 values ranging from 1 to 53 (with an increment of 2 due to the nuclear spin function). As in [2], we have preferred not considering the calculation accounting for the doublet splitting leading to greatly overestimated broadening coefficients for $K = 6$ and 9. The theoretical results from both calculations are presented in Table 2, and the measured and theoretical results are plotted together in Figs. 5 and 6. Note that in Table 2 we list only the theoretical broadenings that correspond to measured coefficients, whereas in the figures we plot all our calculated coefficients.

In Fig. 5, we have plotted both the measured and theoretical results $\gamma(O_2)$ as a function of $|m|$ for selected K transitions in the ^{Q}P-, ^{Q}Q-, and ^{Q}R-branches. For $K = 0, 1, 3, 4$ the results derived from calc. 1 are overestimated, except at low $|m|$ values and $|m| > 12$. They are also significantly larger than the data for higher K values. The second calculation (calc. 2) provides smaller results than calc. 1, and except for $K = 2$ and 4, the agreement with the experimental coefficients is generally improved, especially for $K > 4$ (17.5% for calc. 1 and 7.7% for calc. 2). The measured and theoretical O_2-broadening coefficients, $\gamma(O_2)$, as a function of K for constant $|m|$ are plotted in Fig. 6. It appears that calc. 2 leads to better results than calc. 1 for high $|m|$ values ($|m| > 7$) (13.1% for calc. 1 and 8.3% for calc. 2) and the experimental results generally lie between the results from both calculations for lower $|m|$ values.

4.3. Lineshift coefficients and comparison with experimental data

The O_2-lineshift coefficients $\delta(O_2)$ have been calculated at 296 K for lines in the ^{Q}P-, ^{Q}Q-, and ^{Q}R-branches of the v_2 band. In calc. 1 we have approximated the isotropic part of the potential by a 14-6 LJ model and the vibrational dephasing contribution is obtained by Eq. (9) of [2] where the parameter values $\Delta C_6/C_6 = 0.008$ and $y = 1$ are derived from self-induced lineshifts of CH_3D [1]. In calc. 2 the isotropic potential is a LJ 12-6 model and the vibrational contribution is given by Eq. 3 of [17]. Here the same parameter values for $\Delta C_6/C_6$ and y (0.008 and 1) provide overestimated lineshifts, so we have preferred to use the parameter values obtained from pressure shifts induced by Xe in the v_3 band of CH_3D [18], i.e., $\Delta C_6/C_6 = 0.005$ and $y = 1$. Both series of theoretical results are presented in Table 2 and the measured and theoretical results are plotted together in Figs. 7 and 8. Note that in Table 2 we list only the theoretical shift coefficients that correspond to measured coefficients, whereas in the figures we plot all our calculated coefficients. The results of calc. 2 are systematically smaller in magnitude than the results of calc. 1. Given the scatter of the experimental pressure-induced shifts, $\delta(O_2)$, the comparison with calculated values is rather difficult. Both results are in reasonable agreement with the measurements and from this comparison we cannot have a preference between the two values used for the parameter $\Delta C_6/C_6$.

For each calculation, the results in the ^{Q}R-branch are always smaller in absolute value than those in the ^{Q}P-branch, due to the antisymmetric component in m of the pressure shift derived from the pure rotational contribution. This is not in contradiction with the experimental results which are generally smaller in absolute value in the ^{Q}R-branch than in the ^{Q}P-branch (see Figs. 7 and 8). It should be noted that this rotational contribution corresponding to the half-difference between the results in the P- the R-branches is much smaller in magnitude, even for transitions with K approaching or equal to $|m|$ where it is the strongest, than the vibrational contribution to the shifts given by the results in the Q-branch.

Several interesting trends are revealed in the measured O_2-shift coefficients when they are plotted in Fig. 7 as a function $|m|$ for various K series. The ^{Q}R-branch coefficients for low K show an interesting pattern where they tend from small negative values at low $|m|$ towards more negative values. The pattern exhibits a minimum in the vicinity of $|m| = 8$–11. At higher $|m|$ values the shift coefficients begin to increase towards less negative values. The result is a concave up shape to the graphs. At higher K values the concave up shape is less pronounced and it is followed by a sharply decreasing trend in the shift coefficients at high $|m|$. The ^{Q}P-branch shift coefficients follow a different trend with $|m|$ that appears to be oscillatory. It is difficult to recognize a trend in the ^{Q}Q-branch transitions due to the relatively small number of data points. The theoretical results show reasonable agreement with the experimental shift coefficients (17.0% for calc. 1 and 18.7% for the calc. 2) but they do not seem to reproduce the observed trends in the experimental data.

The O_2-shift coefficients also show interesting trends with K, as revealed in Fig. 8. The ^{Q}R-branch shift coefficients for $|m| = 7$–10 display fairly prominent concave up shapes with minimum around $K = 2$. The theoretical calculations reproduce well the tendency of the ^{Q}R-branch shift coefficients to increase with decreasing K. The general trend in the ^{Q}P-branch shift coefficients is to remain nearly constant for early K values, then to fall off rapidly to more negative values as K approaches $|m|$. This trend is well defined in the theoretical results for the ^{Q}P-branch as well.

5. Conclusion

This paper reports experimental measurements and theoretical calculations of O_2 induced pressure broadening and shift coefficients at room temperature in the v_2 band of the CH_3D molecule. Analyzing 11 FTIR spectra we have measured accurate values for zero pressure line center positions, O_2-broadening coefficients and O_2 pressure-induced shift coefficients for 320 transitions. We have identified several interesting patterns in the measured pressure-broadening and pressure-induced shift coefficients. The empirical expressions derived to compute the O_2-broadening

coefficients as a function of $|m|(|m|+1)$ and K^2 reproduce our measurements to within 4.4%.

The theoretical results of broadening coefficients obtained by considering that the CH_3D molecule is treated as a linear molecule for its interactions with O_2 are very satisfactory. Our calculations can predict the behavior of these broadening with J and K fairly well. We have shown the importance of the isotropic potential governing the trajectory model and the two potentials used lead to results roughly framing the experimental data. The potential derived from molecular LJ parameters provides generally the best agreement with these data. We have shown that the line shifts mainly originate from vibrational dephasing effects. Unfortunately, the measurements of pressure shifts are rather scattered and, therefore, do not allow us to know which of the two kinds of lineshift results is the best and to test accurately our theoretical model.

Acknowledgments

We are very grateful to Dr. Linda R. Brown from the Jet Propulsion laboratory (JPL), California Institute of Technology for allowing us to use her self-broadened CH_3D spectra. Our gratitude also goes to Dr. D. Chris Benner from the College of William and Mary for offering his multispectrum fit program. A. Predoi-Cross acknowledges the support she received from the National Sciences and Engineering Research Council of Canada, University of Lethbridge Research Fund and the Summer Temporary Employment Program of the Government of Canada. The research at the NASA Langley Research Center was performed under contracts with the National Aeronautics and Space Administration. We also thank NASA's Upper Atmosphere Research Program for their support of the McMath-Pierce FTS laboratory facility.

References

[1] A. Predoi-Cross, K. Hambrook, M. Brawley-Tremblay, J.-P. Bouanich, M.V. Devi, D.C. Benner, L.R. Brown, J. Mol. Spectrosc. 234 (2005) 53–74.
[2] A. Predoi-Cross, K. Hambrook, M. Brawley-Tremblay, J.-P. Bouanich, M.A.H. Smith, J. Mol. Spectrosc. 234 (2005) 312–330.
[3] K. Jacquiez, G. Blanquet, J. Walrand, J.-P. Bouanich, J. Mol. Spectrosc. 175 (1996) 386–389.
[4] J. Walrand, G. Blanquet, J.-P. Bouanich, Spectrochim. Acta A 52 (1996) 1037–1040.
[5] G.D.T. Tejwani, K. Fox, J. Chem. Phys. 61 (1974) 759–762.
[6] J.-P. Bouanich, G. Blanquet, J. Walrand, J. Mol. Spectrosc. 161 (1993) 416–426.
[7] E.W. Smith, M. Giraud, J. Cooper, J. Chem. Phys. 65 (1976) 1256–1267.
[8] C. Lerot, J. Walrand, G. Blanquet, J.-P. Bouanich, M. Lepère, J. Mol. Spectrosc. 217 (2003) 79–86.
[9] D. Robert, J. Bonamy, J. Phys. (Paris) 40 (1979) 923–943.
[10] D.C Benner, C.P. Rinsland, V.M. Devi, M.A.H. Smith, D. Atkins, J. Quant. Spectrosc. Radiat. Transfer 53 (1995) 705–721.
[11] R.A. Toth, J. Opt. Soc. Am. B 8 (1991) 2236–2255.
[12] J. Bonamy, L. Bonamy, D. Robert, J. Chem. Phys. 67 (1977) 4441–4453.
[13] J.-P. Bouanich, J. Quant. Spectrosc. Radiat. Transfer 47 (1992) 243–250.
[14] T. Amano, E. Hirota, J. Mol. Spectrosc. 53 (1974) 346–363.
[15] C.G. Gray, K.E. Gubbins, Theory of Molecular Fluids, Oxford University Press, Oxford, 1984.
[16] B. Lance, S. Ponsar, J. Walrand, M. Lepere, G. Blanquet, J.-P. Bouanich, J. Mol. Spectrosc. 189 (1998) 124–134.
[17] J.P. Bouanich, F. Rachet, A. Valentin, J. Mol. Spectrosc. 178 (1996) 157–164.
[18] C. Lerot, G. Blanquet, J.-P. Bouanich, J. Walrand, M. Lepère, Mol. Phys. 103 (2005) 1213–1220.